

RICE UNIVERSITY

**Localization of a swimming robot in a cylindrical  
above-ground tank**

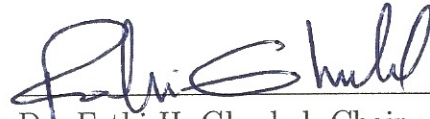
by

**Islem Megdiche**

A THESIS SUBMITTED  
IN PARTIAL FULFILLMENT OF THE  
REQUIREMENTS FOR THE DEGREE

**Master of Science**

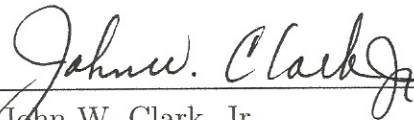
APPROVED, THESIS COMMITTEE:



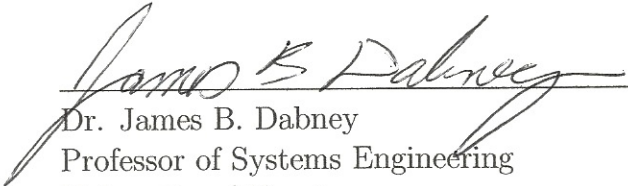
Dr. Fathi H. Ghorbel, Chair  
Professor of Mechanical Engineering



Dr. Marcia K. O'Malley  
Associate Professor of Mechanical  
Engineering



Dr. John W. Clark, Jr.  
Professor of Electrical and Computer  
Engineering



Dr. James B. Dabney  
Professor of Systems Engineering  
University of Houston

HOUSTON, TEXAS

DECEMBER, 2013

# **Abstract**

## **Localization of a swimming robot in a cylindrical above-ground tank**

by

**Islem Megdiche**

Hazardous liquid storage tanks are subject to damage and failure. These tanks need to be inspected for risks of damage. Many systems have been developed for technical inspection of these tanks replacing manual inspection. The use of robots in the field is still an open research problem. Several related issues are not well studied. For example, the navigation of the robot autonomously within the tank which requires the determination of the robot position and the mapping of the environment of the tank. This thesis addresses the planar localization of the robot. First, an overview of the sensors used for the localization of Autonomous Underwater Vehicle is performed leading us to choose the appropriate sensors for the robot in oil tanks. Second, this thesis presents an error analysis study to choose the best number of sensors and their placement that give the most accurate position of the robot. Finally, it addresses the implementation issues of these sensors through several experimental studies.

# Acknowledgements

I would like to express my deep gratitude to my advisor, Dr. Fathi H. Ghorbel, who has been my advisor in every sense of the word. I would like also to thank Dr. James B. Dabney whose guidance is invaluable to the success of my efforts. I thank Dr. John W. Clark, Jr. and Dr. Marcia K. O'Malley for serving on my thesis committee. Thanks to my colleagues and friends, Wissem Jallouli, Imen Mnejja and especially David Trevino and Mohamed Amine Guettat for their help and camaraderie.

I dedicate this work to my parents, Abdellaziz Megdiche and Fatma Smaoui whose efforts and wisdom have guided me through the right path of life, to my brothers and sister, to my intimate friend, Rania Ayadi, and to all the members of my family.

# Table of Contents

<b>Abstract</b>	<b>ii</b>
<b>Acknowledgements</b>	<b>iii</b>
<b>List of Figures</b>	<b>ix</b>
<b>List of Tables</b>	<b>x</b>
<b>1 Introduction</b>	<b>1</b>
1.1 Motivation to this Research . . . . .	1
1.2 Simultaneous Localization and Mapping (SLAM) . . . . .	4
1.3 Problem Formulation . . . . .	7
1.4 Contribution of this Research . . . . .	8
1.5 Outline of this Thesis . . . . .	9
<b>2 Sensors for Swimming Robots</b>	<b>10</b>
2.1 Sensors for Swimming Robots in Unconstrained Environment . . . . .	10
2.2 Types of Tanks . . . . .	18
2.3 Sensors for Robots in Tanks . . . . .	22
2.4 Conclusions . . . . .	25
<b>3 Analytical Sensor Error Analysis</b>	<b>26</b>
3.1 Previous Work . . . . .	26
3.2 Error Analysis . . . . .	29
3.2.1 Localization with Two Sensors . . . . .	30
3.2.2 Localization with Three Sensors . . . . .	40
3.2.3 Localization with Four Sensors . . . . .	42
3.3 Conclusions . . . . .	45

<b>4</b>	<b>Experiment and Results</b>	<b>46</b>
4.1	Objective of the Experiment . . . . .	46
4.2	Design of the Experimental Setup . . . . .	47
4.3	Description of the Experiment . . . . .	50
4.4	Results and Discussions . . . . .	51
4.4.1	First Problem of Interference . . . . .	52
4.4.2	Second Problem of Interference . . . . .	54
4.5	Conclusions . . . . .	64
<b>5</b>	<b>Conclusions and Future Works</b>	<b>65</b>
<b>A</b>	<b>Localization with Two Sensors: <math>\phi = 0^\circ</math></b>	<b>67</b>
<b>B</b>	<b>Localization with Two Sensors: <math>\phi \neq 0^\circ</math></b>	<b>69</b>
<b>C</b>	<b>Experiment 1 with Three sensors</b>	<b>71</b>
<b>D</b>	<b>Experiment 1 with Four sensors</b>	<b>73</b>
	<b>Bibliography</b>	<b>78</b>

# List of Figures

1.1	Localization Problem . . . . .	5
1.2	Mapping Problem . . . . .	5
1.3	Simultaneous Problem . . . . .	6
2.1	Earth Magnetic Field . . . . .	13
2.2	Compass Tilt . . . . .	14
2.3	Case of Absence of Ferrous Material . . . . .	15
2.4	Case of Existence of Ferrous Material . . . . .	15
2.5	Draper Tuning Fork Gyroscope . . . . .	17
2.6	Piezoelectric Plate Gyroscope . . . . .	17
2.7	Fixed Roof Tank . . . . .	19
2.8	External Floating Roof Tank . . . . .	20
2.9	Internal Floating Roof Tank . . . . .	20
2.10	Domed External Floating Roof Tank . . . . .	21
2.11	Problem of GPS Signal in Reaching the Robot . . . . .	23
2.12	Proximity Sensor . . . . .	24
3.1	Robot in Oil Tank . . . . .	27
3.2	Localization with the First Sensor . . . . .	27
3.3	Localization with the Second Sensor . . . . .	28
3.4	Localization with the Third Sensor . . . . .	29
3.5	Error Mapping in Case of Zero Error in Sensors . . . . .	31
3.6	Error Mapping in Case of Error in Sensors . . . . .	32
3.7	Error Mapping for the Case $\theta_2 = 180$ degrees . . . . .	32
3.8	Error Mapping for the Case $\theta_2 = 40$ degrees . . . . .	33
3.9	Maximum Error Distance $\rho$ . . . . .	33

3.10	Sensors . . . . .	34
3.11	Tank Contour . . . . .	34
3.12	Nominal Point and Sensor Readings . . . . .	35
3.13	Nominal Circles of the Two Sensors . . . . .	35
3.14	Position Error . . . . .	36
3.15	Simulation Case Study . . . . .	37
3.16	First Case . . . . .	38
3.17	Second Case . . . . .	38
3.18	Two Sensors: $\phi = 0^\circ, \theta_2 = 270^\circ$ . . . . .	39
3.19	Two Sensors: $\phi = 40^\circ, \theta_2 = 310^\circ$ . . . . .	39
3.20	Error Area Given by Three Sensors . . . . .	40
3.21	Three Sensors: $\phi = 0^\circ, \theta_2 = 90^\circ, \theta_3 = 180^\circ$ . . . . .	41
3.22	Three Sensors: $\phi = 0^\circ, \theta_2 = 120^\circ, \theta_3 = 240^\circ$ . . . . .	41
3.23	Three Sensors: $\phi = 20^\circ, \theta_2 = 110^\circ, \theta_3 = 200^\circ$ . . . . .	41
3.24	Three Sensors: $\phi = 40^\circ, \theta_2 = 130^\circ, \theta_3 = 220^\circ$ . . . . .	41
3.25	Three Sensors: $\phi = 10^\circ, \theta_2 = 130^\circ, \theta_3 = 250^\circ$ . . . . .	42
3.26	Three Sensors: $\phi = 70^\circ, \theta_2 = 190^\circ, \theta_3 = 310^\circ$ . . . . .	42
3.27	Four Sensors: $\phi = 0^\circ, \theta_2 = 90^\circ, \theta_3 = 180^\circ, \theta_4 = 270^\circ$ . . . . .	43
3.28	Error Area Given by Four Sensors . . . . .	43
3.29	Four Sensors: $\phi = 30^\circ, \theta_2 = 120^\circ, \theta_3 = 210^\circ, \theta_4 = 300^\circ$ . . . . .	44
3.30	Four Sensors: $\phi = 40^\circ, \theta_2 = 130^\circ, \theta_3 = 220^\circ, \theta_4 = 310^\circ$ . . . . .	44
3.31	Four Sensors: $\phi = 50^\circ, \theta_2 = 140^\circ, \theta_3 = 230^\circ, \theta_4 = 320^\circ$ . . . . .	44
4.1	The Experimental Setup . . . . .	47
4.2	Rod . . . . .	48
4.3	Higher Positioning Plate . . . . .	49
4.4	Platform . . . . .	49
4.5	Electronic Board . . . . .	50

4.6	Experiment 1 with 3 Sensors . . . . .	51
4.7	Experiment 1 with 4 Sensors . . . . .	51
4.8	Experiment 1 with Three Sensors: Sensors 1 and 2 . . . . .	53
4.9	Experiment 1 with Four Sensors: Sensors 1, 2, 3 and 4 . . . . .	54
4.10	Experiment 2 with Three Sensors Giving Stable Measurements . . . . .	57
4.11	Matlab Window Showing Stable Measurements with Three Sensors . . . . .	58
4.12	Experiment 2 with Three Sensors Giving Unstable Measurements . . . . .	58
4.13	Matlab Window Showing Unstable Measurements with Three Sensors . . . . .	59
4.14	Experiment 2 with Four Sensors Giving Stable Measurements . . . . .	59
4.15	Matlab Window Showing Stable Measurements with Four Sensors . . . . .	60
4.16	Experiment 2 with Four Sensors Giving Unstable Measurements . . . . .	60
4.17	Matlab Window Showing Unstable Measurements with Four Sensors . . . . .	61
4.18	Error Area . . . . .	61
4.19	Intersection of the Circles . . . . .	62
4.20	Possible Locations of the Platform . . . . .	62
4.21	Stability and Instability Areas . . . . .	63
4.22	Signal Reflection . . . . .	64
A.1	Two Sensors: $\phi = 0^\circ, \theta_2 = 20^\circ$ . . . . .	67
A.2	Two Sensors: $\phi = 0^\circ, \theta_2 = 45^\circ$ . . . . .	67
A.3	Two Sensors: $\phi = 0^\circ, \theta_2 = 90^\circ$ . . . . .	67
A.4	Two Sensors: $\phi = 0^\circ, \theta_2 = 140^\circ$ . . . . .	67
A.5	Two Sensors: $\phi = 0^\circ, \theta_2 = 180^\circ$ . . . . .	68
A.6	Two Sensors: $\phi = 0^\circ, \theta_2 = 220^\circ$ . . . . .	68
A.7	Two Sensors: $\phi = 0^\circ, \theta_2 = 270^\circ$ . . . . .	68
A.8	Two Sensors: $\phi = 0^\circ, \theta_2 = 300^\circ$ . . . . .	68
B.1	Two Sensors: $\phi = 30^\circ, \theta_2 = 190^\circ$ . . . . .	69
B.2	Two Sensors: $\phi = 50^\circ, \theta_2 = 210^\circ$ . . . . .	69

B.3	Two Sensors: $\phi = 70^\circ$ , $\theta_2 = 230^\circ$ . . . . .	69
B.4	Two Sensors: $\phi = 20^\circ$ , $\theta_2 = 290^\circ$ . . . . .	69
B.5	Two Sensors: $\phi = 40^\circ$ , $\theta_2 = 310^\circ$ . . . . .	70
C.1	Experiment 1 with Three Sensors: Sensors 1 and 3 . . . . .	71
C.2	Experiment 1 with Three Sensors: Sensors 1, 2 and 3 . . . . .	72
D.1	Experiment 1 with Four Sensors: Sensors 1 and 2 . . . . .	73
D.2	Experiment 1 with Four Sensors: Sensors 1 and 3 . . . . .	74
D.3	Experiment 1 with Four Sensors: Sensors 1 and 4 . . . . .	74
D.4	Experiment 1 with Four sensors: Sensors 1, 2 and 3 . . . . .	75
D.5	Experiment 1 with Four Sensors: Sensors 1, 2 and 4 . . . . .	75
D.6	Experiment 1 with Four Sensors: Sensors 1, 3 and 4 . . . . .	76

# List of Tables

- 4.1 Experiment 2 with Three Sensors . . . . . 55
- 4.2 Experiment 2 with Four Sensors . . . . . 56

# Chapter 1

## Introduction

Above Storage Tanks (AST) are large vessels that contain organic liquids. They are used in many industries such as petrochemical and chemical manufacturing, petroleum producing and refining, bulk storage, transfer operations and many other industries [1]. These tanks are liable to damages and collapses that might have dramatic consequences. In this Chapter, we are firstly going to review the causes of these damages, their consequences and the methods adopted to ensure the safety of the tank manually and automatically. We are secondly going to present Simultaneous Localization and Mapping (SLAM) as a research area related to the automatic inspection of the tank. We are going finally to address the problem that this thesis tries to solve, present the contributions to this research and the outline of this thesis.

### 1.1 Motivation to this Research

During the long period of the exploitation of Above Storage Tanks, many types of damages occur such as deviation of design geometric shape which is characterized by a local or total loss of stability, a deviation of shell and bottom and bending of annular bottom plates. Another type of damage that may affect AST is the occurrence of cracks. They are fissures that can be found in weld seams and steel structures. Due to vibration and static stress, they can be enlarged causing serious failures. AST are also subject to corrosion and metal degradation which attack both welds and steel structures [2]. These damages have harmful effects on human beings, ecology and economy. One of the biggest hazards is the explosion resulting from the evaporative losses if tanks are not well sealed. In addition, due to the

huge dimensions of the tanks that are filled with chemical, their bottoms are subject to enormous weight. That can cause leakage resulting in the destruction of water bodies. Around the world, there have been several storage tanks ruptured resulting in dramatic consequences. Here are listed some of the incidents that happened in the US.

- Tank Collapse (Iowa 1997) [2]: A 1- million gallon tank that contains ammonium collapsed and released the product. The walls of this tank fell onto two other tanks causing the breaking of its valves and the release of its content. Fortunately, much of the release was trapped by a dike but building another dike was necessary to prevent the product to flow into the Missouri River.
- Tank Rupture (Ohio 2000) [2]: A 1-million gallon tank containing liquid fertilizer ruptured and triggered damages to four neighboring reservoirs. The liquid flow broke a dike wall and hit five tractor-trailer rigs, two out of them were pushed into the river. A big quantity of the released liquid was spread into the Ohio River increasing the algae growth.
- Tank Rupture (Ohio 2000) [2]: A 1.5 million gallon tank of ammonium phosphate collapsed and caused the rupture of three nearby tanks that held phosphoric acid and magnesium chloride mixture causing them to leak. The released liquid flowed into nearby creeks. This dramatic incident caused the evacuation of a neighboring school and forced the public to drink the bottled water since the water supply is contaminated by the spilled chemicals.
- Tank Explosion (Delaware 2001) [3]: Sparks from hot work on a catwalk above one of the tank on the site entered a large sulphuric acid tank through corrosion holes causing an entire explosion. Due to the flammable vapors and subsequent ignition, the tank shell was propelled away and approximately 660.000 gallons of acid was released. This accident caused the death of one worker, the injury of eight others and a big environmental damages including killing thousands of fishes and other wildlife.

Many factors trigger the failure of the previously listed Above Storage Tanks. It appears that the main factor is the defective weld. In addition, tanks holding chemicals are more subject to failure because they contain hazardous materials. Failure is caused by the age of the tank, the occurrence of corrosion around the base and direct contact with the ground that may result in the leakage [2]. Tanks could also collapse due to the high wind, lightning and frequent precipitation. In order to reduce the possible hazards, some steps have to be taken into consideration such as design and construction of the tank according to the norms, maintenance and inspection. The inspection and diagnosis aims at determining zones joints, examining tank walls, assessing corrosion damages, measuring the real thickness of the shell and checking status of seals.

Currently, inspection is carried out manually. In this case, the tank must be out of service for few weeks which is translated into a substantial monetary operational expenditure for the owner/operator. If the operation concerns the internal corrosion and the tank bottom, the facility has to be emptied, cleaned and vented. This process is highly time consuming, tedious, labor intensive and expensive. Furthermore, the operator is exposed to toxic materials which puts his life in risk. As a part of the ongoing efforts to protect the operator and to reduce the economical consequences of the manual inspection, researchers suggested to use robots. These robots use Ultrasonic Testing (UT) instrumentation to appraise tank structures, providing more reliable results in less time. Besides, the use of robots allows to inspect the facility while in service without shutting it down. Moreover, it reduces personal exposure to toxic waste materials [4].

However, the application of inspection robots in oil storage industry is still a new field to which many challenges are related. Therefore, it becomes indispensable to design modern robotic systems that account for the quality of inspection, effects of environment (pressure, temperature, humidity, etc), requirements of autonomy and the ability of navigation. The latter denotes the vehicle's capacity to establish its own position with respect to a frame of references and to reach some goal locations. Simultaneous Localization and Mapping (SLAM) is an area of robotics research that has the purpose of ensuring the navigation.

It deals with the problem of building a map of an unknown environment by a robot while simultaneously using this map to navigate in the environment. The following section gives a brief introduction to Simultaneous Localization and Mapping (SLAM). It explains the concept, its parts and steps.

## 1.2 Simultaneous Localization and Mapping (SLAM)

Simultaneous Localization and Mapping deals with the problem of building a map of an unknown environment by a robot while simultaneously using this map to localize itself [5]. The process of SLAM is constituted of two main parts: localization and mapping.

The localization consists of determining the robot's pose to describe how the robot is positioned, as shown in Figure 1.1. For a planar problem, the pose is a vector that contains  $x$  and  $y$  coordinates and the orientation  $\theta$

$$X = \begin{bmatrix} x \\ y \\ \theta \end{bmatrix} . \quad (1.1)$$

For a spatial problem, the vector contains  $x$ ,  $y$  and  $z$  coordinates along with the roll, yaw and pitch angles

$$X = \begin{bmatrix} x \\ y \\ z \\ \phi \\ \theta \\ \psi \end{bmatrix} . \quad (1.2)$$

The robot pose is determined with respect to references called also landmarks or features. Features can be placed artificially or can be naturally occurring cracks or corners. In all cases, features have to be distinguishable which means that robots can detect their sizes, colors or shapes.

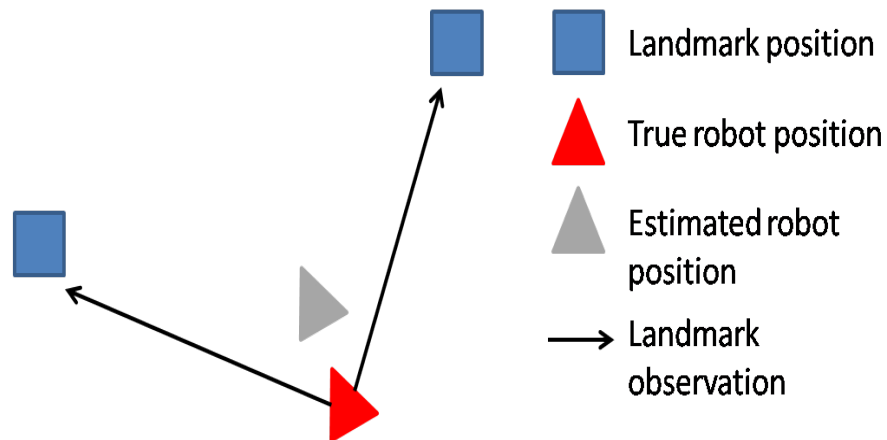


**Figure 1.1:** Localization Problem

The mapping part focuses on the determination of the absolute locations of the features assuming the robot knows its position, as shown in Figure 1.2. This part generates in the end a map containing the estimates of landmarks' location. When the robot moves, the latter re-locates the features and updates the map with the new estimates.

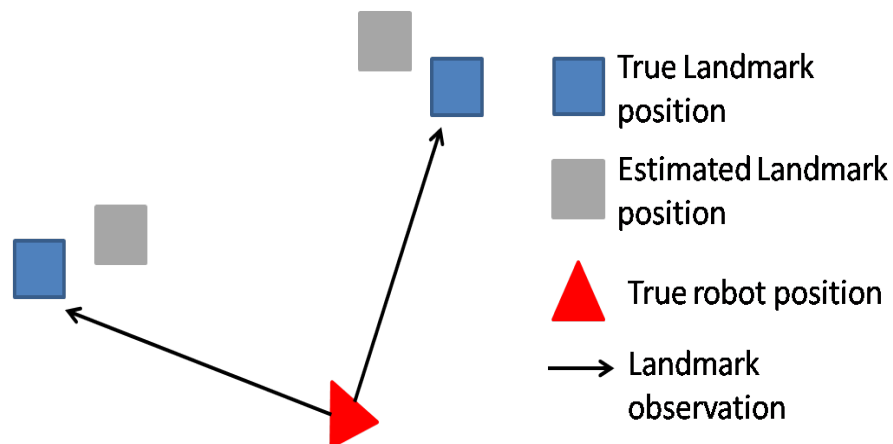


**Figure 1.2:** Mapping Problem

As a conclusion, in the localization process, the robot needs the map of the environment to determine its position and in the mapping process, the map is generated from the robot's position. So the input of each process is the output of the other, that is why we use SLAM, as shown in Figure 1.3.

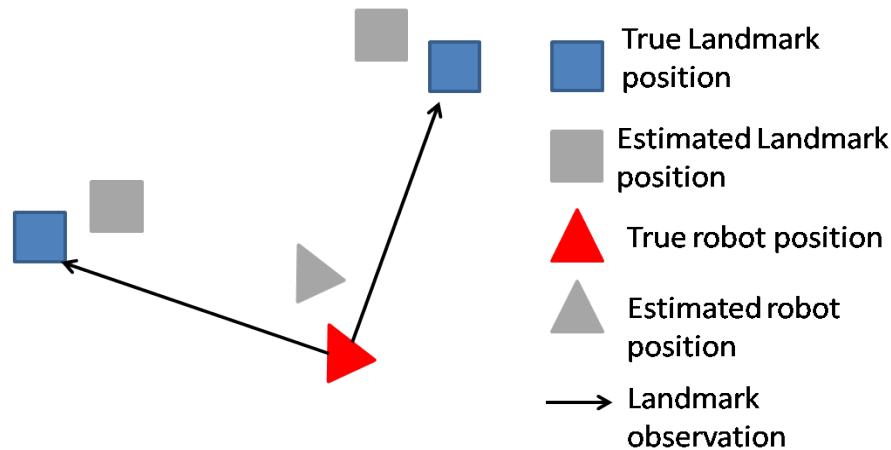


**Figure 1.3:** Simultaneous Problem

SLAM consists of the following steps: Firstly, the robot extracts the utilized landmarks from its sensory inputs. Secondly, it associates the observed landmarks from different sensors with each other, in other words, if a landmark is observed and then re-observed, the robot has to know that it is the same one. Then, it estimates the state. After that, the robot updates the state by re-observing the landmarks and using the estimates of the current position to estimate the landmarks locations. Finally, the landmarks locations will be updated by adding them to the state.

SLAM is a domain that dated back to the mid of 1980 and is still a challenging area of research. It is very useful in many areas that are hazardous or inaccessible such as deep seas or unstable structures by providing maps that may be helpful to understand the geological sites or to localize defects in tanks and pipelines. It also allows the navigation in unknown environments like space stations and other planets. Its application in the domain of oil tank inspection is very interesting. But, it has received little attention in previous works. In fact, only a handful of references in the literature treated that problem and mainly the localization of Autonomous Underwater Vehicle in unstructured environment was the focus of the prior researches. The next section introduces the problem that this thesis tries to solve and the related challenges.

## 1.3 Problem Formulation

The main problem addressed by this thesis is to study the localization part of the SLAM problem. For example, during the inspection of the facility, the robot would navigate through the tank, and would be able to answer the question, “Where am I?” based on the measured sensor data. However, this application has its specific constraints that require a comprehensive analysis in order to make the good choice of sensors. Broadly, these constraints include the nature of medium where the robot is operating. It can be oil or chemical that is a flammable fluid. So, there exists a risk of explosion. Another constraint is that the tank is constructed from metallic sheets which are good reflectors of signals. Therefore, they might distort the measured sensor data. Furthermore, the size of the robot is an important factor which helps to decide on the suitable sensors to be used. Once the sensor choice is done, it is necessary then to decide on their number and their placement. This decision is not done at random and it should follow a systematic approach. That is why, apart from selecting the appropriate sensors, this work aims at establishing a rigorous framework within which the number and placement choice of sensors is done based on the analytical error analysis. This problem may be decomposed into a number of steps:

The first step is to look in the literature for the sensors used for the localization of Autonomous Underwater Vehicle since this application is the nearest to the use of robots in oil tanks. Then, understanding of how they work and what are their limitations. The second step is to select the sensors for position measurements as well as rotation measurements. The third step deals with the determination of the optimal number of sensors that leads to more accurate data. A way to do that is to adopt the error in position as a measure of goodness. Given a nominal point that defines the location of the robot inside the tank, the estimated location from the sensors is calculated. Due to the uncertainty in sensors combined with the noise and error calculation that result from the electronic board connecting the sensors to the computer, the calculated value will deviate from the nominal one. The extent to which it will deviate is a major question that needs

to be answered. This deviation is postulated to depend on the number of sensors and the relative angle between them. The fourth step is to conduct an experiment using the chosen sensors to test implementation issues such as the reflection and interference between the signals and to see how much they can affect the accuracy of the results. The next section discusses the contributions of this work in light of the problem formulation.

## 1.4 Contribution of this Research

The previous section presented the main problem and the related issues. This section discusses how this thesis addresses these issues and contributes to solving that problem.

- The first contribution of this thesis is to choose the appropriate sensors respecting all the constraints in oil tanks. This will be done through a literature review of sensors.
- Second, it is significant to conduct a whole study based on error analysis. The literature review indicates that almost all the work on the Simultaneous Localization and Mapping (SLAM) for Autonomous Underwater Vehicle (AUV) or for robots in oil tank did not follow an approach to choose the number of sensors. In contrast, this work aims to determine the optimal number of sensors used to calculate the position as well as the relative angle between them through several simulations. This approach is not only limited to this application but could be used in other problems where optimality is desired.
- The third contribution is to conduct an experiment through which implementation issues of interference between signals and reflection are studied. This experiment will demonstrate the impact of using a circular tank on the accuracy sensor readings. It also explains how deeply the relative angles between the sensors can affect the measurements.

## 1.5 Outline of this Thesis

This thesis is organized as follows: Chapter 2 describes the SLAM problem in oil tank. It first reviews the sensors used for swimming robots in unconstrained environment. It then discusses whether they are suitable for the application of robots in oil tanks. It describes the types of tanks and their parts that need to be inspected. Finally, it justifies the selected sensors. Chapter 3 describes the error analysis study using first two, second three and finally four sensors. Several simulation results illustrate each study case. Likewise, Chapter 4 presents the experiment conducted to test implementation issues which are the reflection and the interference. It first describes the set up. Then, it details the results. Finally, it discusses them. Finally, Chapter 5 provides a conclusion of the study.

# Chapter 2

## Sensors for Swimming Robots

This Chapter enumerates the sensors used for Autonomous Underwater Vehicles and discusses its compatibility for swimming robots in oil tanks and also describes components of the tank that need to be inspected.

### 2.1 Sensors for Swimming Robots in Unconstrained Environment

In order to decide on the suitable sensors to be used for robots in oil tank, an investigation of sensors used for Autonomous Underwater Vehicle in unconstrained environments was carried since it is the closest to that problem. These sensors include (Global Positioning System) GPS, (Inertial Navigation System) INS, Imaging Sonar, Visual-based Sensor, Underwater Acoustic System, Magnetic Compass, Gyroscope, Gyrocompass and Microelectromechanical Systems (MEMS) Gyroscope.

**Global Positioning System:** GPS provides the location and time information of any object which receives radio signals broadcasted by satellites installed by US Department of Defense. The main drawback when using a GPS system is that it is not possible to determine the location of the object where there is not a line of sight to four or more satellites. The GPS is useless in case the object is near skyscrapers or inside a tunnel [6]. Similarly, for an (Autonomous Underwater Vehicle) AUV, the workspace of a GPS is limited to shallow water. For robots inside an oil tank, GPS cannot determine robot's

location when it is swimming near the bottom mainly because the oil tank is very large with a height reaching 50 *m*. Indeed, for such locations within the tank where the signal emitted from the satellites cannot reach the GPS receivers, the robot cannot localize itself. This is because radio signal indicating information about the satellite position and timing data may not penetrate the shell of the tank. And even it does, it will be weakened by the liquid before it reaches the receiver.

**Inertial Navigation System:** INS is the acronym of Inertial Navigation System. It uses accelerometers and gyroscopes to calculate the position, orientation and velocity of an object. INS is usually integrated with GPS to ensure the accuracy since it compensates for the intermittent reception of signals. The combined system is often used in planes, ships or mobile robots, etc [6]. INS may not be suitable to be incorporated on the swimming robot in oil tank for two reasons: The first one is because its size is bigger than the robot size. The second one is because it is usually integrated with GPS which is inappropriate to our application.

**Side Imaging Sonar:** Side Imaging Sonar called also Side Scan Sonar and Bottom Classification Sonar is a type of sonar systems that is basically used to take images of the sea floor. The device emits a pulse. When the latter bounces off of an object, an echo is returned and sent to a computer or a console to display the resulting image. One of the advantages of this system is the rich information which lead to high accurate position. However, this system is not free from drawbacks since the power energy is so important and its volume is so big [6] therefore it cannot be fixed on small robots.

**Visual-based Sensor:** Visual-based Sensor includes Video Camera and Laser-based Vision System. Both of them are cheap and have good informative character. However, the Laser-based Vision System has some other advantages. It has a very strong laser beam so it cannot be easily weakened by water. Besides, it is not sensitive to low visibility and bad lighting conditions. In contrast, the Video Camera suffers from this problem, therefore,

its range is too short [6].

**Underwater Acoustic Positioning System:** This system is widely used in sea-floor exploration and marine archeology. The position of the AUV is determined relative to a framework of baseline stations. Underwater Acoustic Positioning Systems contain four classes which are Long Baseline (LBL) System, Short Baseline (SBL) System, Ultra Short Baseline (USBL) System and GPS Intelligent Buoys(GIB) [6].

- Long Baseline (LBL) System: It uses a sea floor baseline transponder network. This category is known with its accurate and robust position.
- Short Baseline (SBL) System: Unlike the Long Baseline (LBL) System, SBL system uses three or more transducers fixed in the bottom of a ship. The accuracy obtained depends on the way of mounting the transducers.
- Ultra Short Baseline (USBL) System: Unlike the LBL and the SBL that calculate the position measuring multiple distances, USBL uses only one transducer and determines the position of the AUV by measuring the distance and the direction. However, this type suffers from a low level of robustness and accuracy.
- GPS Intelligent Buoys (GIB): This type is almost similar to LBL System with some differences. Instead of deploying the transducers in the bottom of the seafloor, the transducers are replaced by floating buoys which are positioned by GPS fixed on a ship. The AUV measures its position by measuring the time of travel of the signal from the AUV to the buoys.

Underwater Acoustic Positioning System is a good option to localize the robot inside the tank since it uses acoustic signals that propagate well in water. The acoustic signals propagate better in oil because the oil viscosity is less than water viscosity. But, it has some drawbacks since it requires fixing transponders in the bottom of the tank in case of (LBL) System or they also can be fixed on the bottom of a ship when using (SBL) or

(USBL) Systems. The use of (GIB) System requires also the use of a ship to fix the GPS. This may be impractical inside the tank.

**Magnetic Compass:** The compass is an ancient tool used by earlier navigators. It is still used at the present but it has been developed leading to the electronic compass. The latter involves two types of sensors [7]. The first type is the fluxgate sensor, it consists of a set of coils around a core. The magnetic field is measured with the help of an excitation circuitry. This type of sensor can output readings with less than 1 milligauss resolution. However, it is bulky, fragile and has a low response time. The second type is the magnetoresistive sensor which is made of thin strips of permalloy (NiFe magnetic film). The value of the magnetic field is determined through the measurement of the film's resistance. This type is better than the fluxgate sensor, it has a small sensitivity below 0.1 milligauss, a small size and outputs readings within 1 microsecond. The electronic compass works on the basis of the calculation of the horizontal components of the earth magnetic field  $H_X$  and  $H_Y$  (see Figure 2.1) to give the value of the heading called also azimuth or yaw angle

$$Azimuth = \frac{H_Y}{H_X}. \quad (2.1)$$

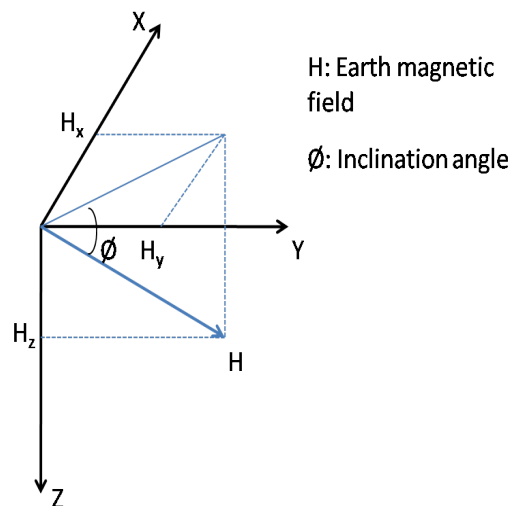


**Figure 2.1:** Earth Magnetic Field

In case object holding the compass is not in the horizontal plane, as shown in Figure 2.2, it is required to determine the pitch and roll angles in order to calculate the heading.

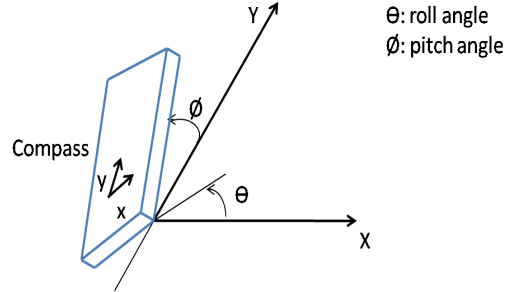


**Figure 2.2:** Compass Tilt

These angles are determined with a tilt sensor or an inclinometer. There are two main types of tilt sensors. The first category is filled with liquid and uses electrodes to control the movement of liquid when the angles vary. The second one uses accelerometer that calculates the earth's gravitational field using an electromechanical circuit and gives electrical signal proportional to the tilt angles. Using these following equations,

$$H_X = X \cos \phi + Y \sin \theta \sin \phi - Z \cos \theta \sin \phi, \quad (2.2)$$

$$H_Y = Y \cos \phi + Z \sin \theta, \quad (2.3)$$

and

$$Azimuth = \frac{H_Y}{H_X} \quad (2.4)$$

we calculate the heading where  $X$ ,  $Y$  and  $Z$  are the magnetic readings.

In addition to the tilt compensation, the electronic compass is able to compensate the effects of ferrous material. If there is no ferrous material, the curve presenting the horizontal magnetic field component along the  $Y$  axis as a function of the horizontal magnetic field along the  $X$  axis, shown in Figure 2.3, is a circle centred around the origin.

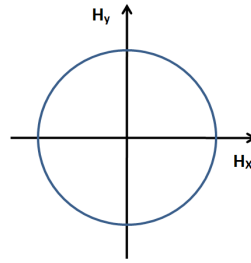


**Figure 2.3:** Case of Absence of Ferrous Material

When the compass is near ferrous material, there is a distortion of the curve shape. This means that the shape will change into an ellipsoid form and the center of the circle will shift, as shown in Figure 2.4.

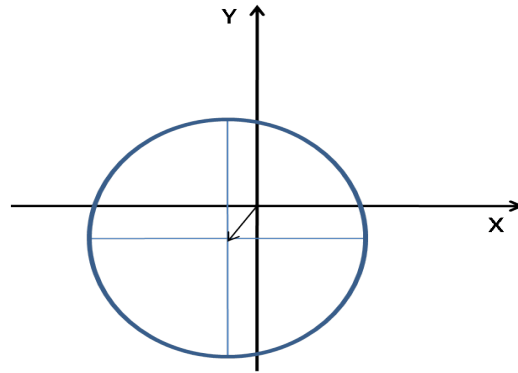


**Figure 2.4:** Case of Existence of Ferrous Material

In order to compensate the effects of the ferrous material, it is necessary to determine two scale factors  $X_{sf}$  and  $Y_{sf}$  to bring back the circular form of the curve and two offset factors  $X_{off}$  and  $Y_{off}$  to transfer the circle's center to the origin.

The electronic compass has some other advantages, it is resistant to vibration and shock and can be directly interfaced with electronic navigation system. The compass is a suitable choice for the localization of the robot in oil tank for many reasons: First, its size is small so it can be fixed on the robot. Then, the metallic tank does not affect the reading thanks to the ferrous material compensation property. Finally, it can determine the orientation of the robot even when it is tilted.

**Gyrocompass:** The gyrocompass is a navigational instrument similar to the gyroscope. The classical one uses a spinning wheel that finds the direction of the true north [8]. This device is able to work near ferrous materials without affecting the reading. It is used in ships, planes and spacecrafts. The gyrocompass can be numeric and is used in rockets. But, it is not suitable to be used for robots due to its big size.

**Gyroscope:** The first type of gyroscope was invented in the early 1800's [9]. It uses a spinning wheel based on the principle of angular momentum to determine the orientation. It is used for navigation of ships and planes by measuring the angle of rotation. It is also used in the control. A mechanical gyroscope suffers from the problem of wear and it is big in size, therefore it is not suitable to be used for robot in oil tank. The second type is the optical gyroscope, it appeared in the 1960's. It works on the basis of sending two laser beams around a circular path following opposite directions. The beam moving against the rotation has a shorter path than the path of the second beam. The resulting phase shift is measured and hence the value of the rotation angle is calculated. The optical gyroscope is used in aeronautics and military applications. It is more reliable than the mechanical gyroscope thanks to its size and weight and mainly because it does not suffer from the problem of wear.

**MEMS Gyroscope:** The acronym of Microelectromechanical Systems Gyroscope, MEMS gyroscope was invented in the last few years and realized many advancements over the gyroscopes mainly in its size. Some MEMS Gyroscopes are discussed in below [9].

- Draper Tuning Fork Gyroscope: It consists of two tines (see Figure 2.5); the rotation of the tines which results in the creation of Coriolis force which itself causes a perpendicular force to the tines. This force causes a bending of the tuning fork which is proportional to the rate of the rotation.

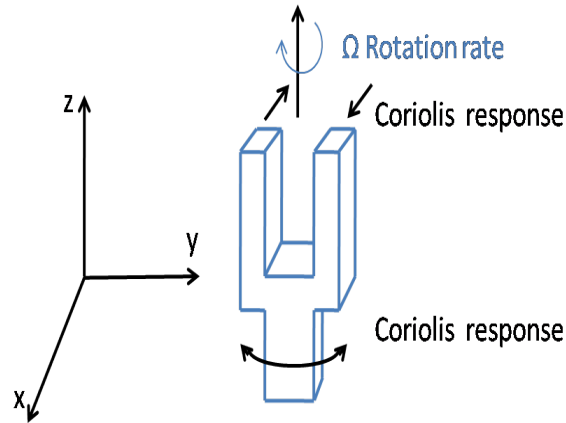


**Figure 2.5:** Draper Tuning Fork Gyroscope

The first Draper Tuning Fork Gyroscope was developed in 1993 and is used in the automobile industry as a yaw rate sensor for skid control in anti-lock braking applications.

- Piezoelectric Plate Gyroscope: This type of gyroscope uses a piezoelectric material that vibrates when it receives a voltage and gives a voltage when it is subject to a force. The plate has six electrical leads on its sides through which the plate is provided with voltage and the outputs are measured (see Figure 2.6).

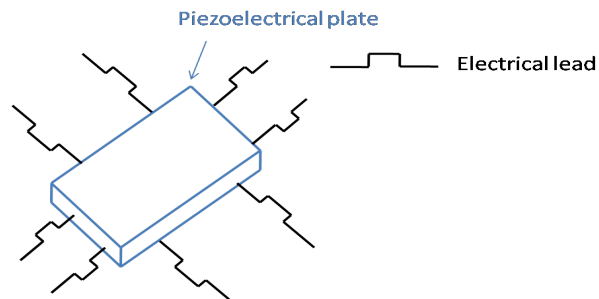


**Figure 2.6:** Piezoelectric Plate Gyroscope

In case the object holding this type of gyroscope is rotating about a perpendicular axis to the drive voltage, a voltage which is proportional to the angular velocity is

created in the third perpendicular direction. The Piezoelectric Plate Gyroscope is useful because it does not require a high voltage to give readable outputs. Besides, it can measure the rotation in two directions. In case the drive voltage is switched, it can measure the rotation in the third direction.

MEMS Gyroscopes are the best option for robots in oil tanks for many reasons: First, they are not affected by ferrous materials. Second, their small size allows them to be integrated in the robot. Finally, they can support mechanical damage, harsh environment and contamination since they are enclosed in packages made from pyrex [10]. These packages are sealed using the anodic and eutectic bonding at high temperature.

After reviewing the sensors used for Autonomous Underwater Vehicle, it is necessary to review the types of oil tanks and to decide on the particular parts of the tanks that should be inspected.

## 2.2 Types of Tanks

Above ground storage tanks are used to store chemicals and petroleum products. They are constructed from metallic plates welded together. They have big dimensions reaching  $20m$  in height and  $50m$  in diameter. There are six basic tanks designs [1].

**Fixed Roof Tank:** Fixed Roof Tank can be horizontal or vertical. For the vertical one, shown in Figure 2.7, it has cylindrical steel shell with an affixed roof. The shape of the roof varies from one tank to another. It can be conical, domical or flat. One of the drawbacks of this type is that it allows evaporative losses of the stored liquid due to change in temperature, pressure and liquid level.

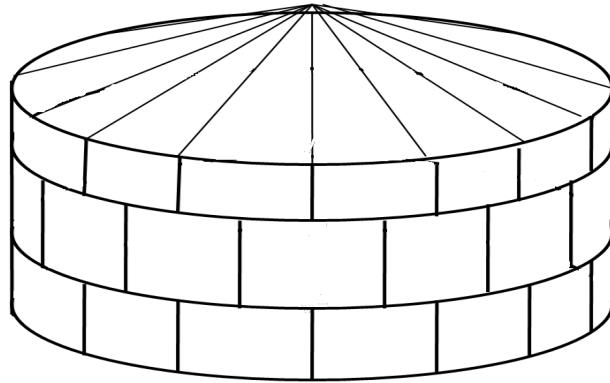


**Figure 2.7:** Fixed Roof Tank

The second subtype of that family is the horizontal tank. It is composed of both above-ground and underground services. Unlike the vertical tank, the horizontal is almost elliptical and its length has not to exceed six times the diameter in order to ensure the structural integrity.

**External Floating Roof Tank:** External Floating Roof Tank (EFRT), as shown in Figure 2.8, consists of an open-topped cylindrical steel shell containing a floating roof that moves up and down relative to the change of the liquid level. The floating roof consists of deck fittings and rim seal system. There are two main types of decks: pontoon and double-deck. Whatever the design of the roof is, the purpose of that type of tank is to reduce the volatile organic compounds. But, the main drawback of this type of tank is that rain water can accumulate on the roof.

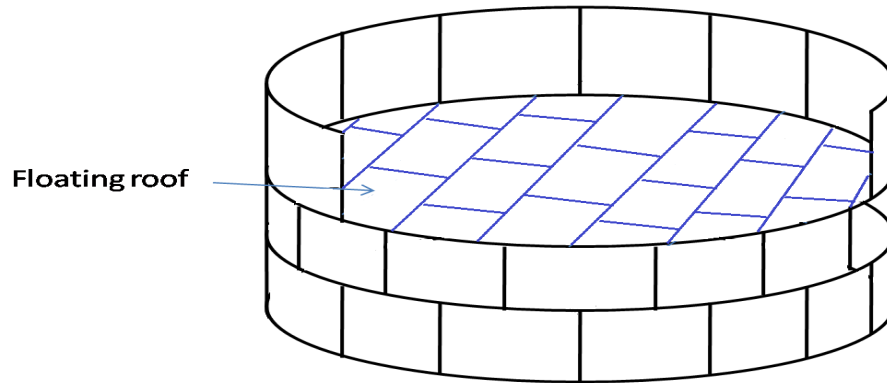


**Figure 2.8:** External Floating Roof Tank

**Internal Floating Roof Tank:** Internal Floating Roof Tank (IFRT) is a type that combines between both fixed roof tank and external roof tank. It is composed of a permanent roof where a floating roof inside, as shown in Figure 2.9. There are two main categories of the internal floating roof tanks:

- Tank with a fixed roof supported by vertical columns: This type was designed first to be a fixed roof tank and then retrofitted to be internal floating roof tank.
- Tank with a self-supporting fixed roof and no internal support columns: Unlike the previous type, this one was originally an external floating roof and then converted to an internal floating roof.

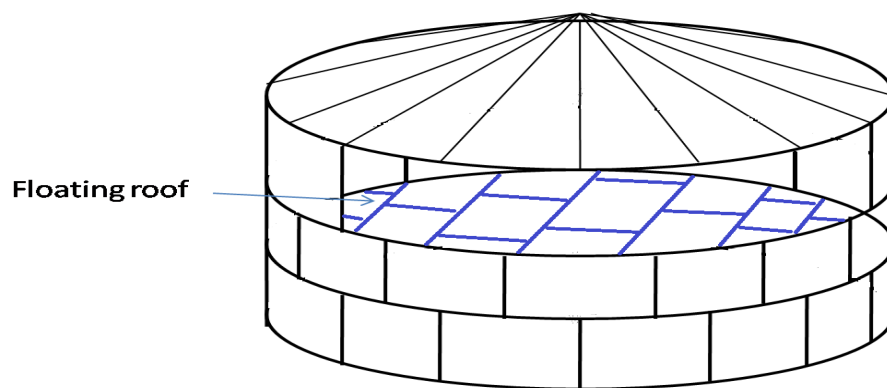


**Figure 2.9:** Internal Floating Roof Tank

**Domed External Floating Roof Tank:** This type of tank comes from retrofitting an existing external floating roof tank with a domed roof. It has the heavier deck to block the wind. Domed external floating roof tank is similar to internal floating roof tank, as shown in Figure 2.10. It has a welded deck and a self supporting fixed roof.

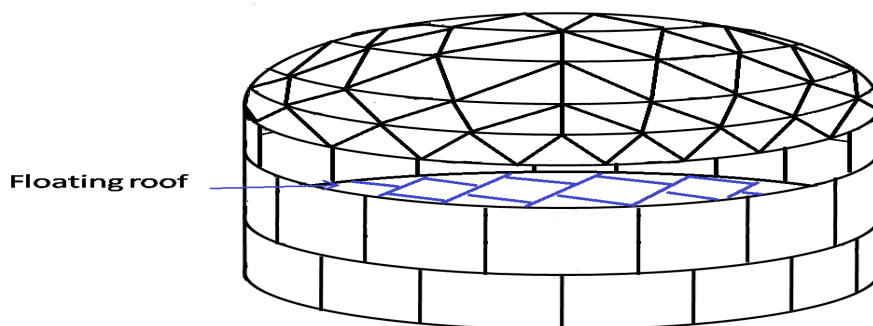


**Figure 2.10:** Domed External Floating Roof Tank

**Variable Vapor Space Tank:** This type has an expandable vapor reservoirs to accommodate the fluctuations of vapor volume due to change in temperature and pressure. There are two basic categories of variable vapor space tanks: lifter roof tanks and flexible diaphragm tanks. The former use telescoping roof that fits loosely around the main tank wall. They use a seal to close the space between the wall and the roof. The latter use flexible membranes to provide expandable volume.

**Pressure Tank:** This type of tank is devoted to store the organic liquid and gases with high vapor pressure. However, they can only be used for the products with low pressure that goes from 2.5 to 15 psig. This type is available in different shapes that depend on the operating pressure.

All the tanks listed above contain rim seal which is used to deal with the problem of emission caused by the evaporative losses. The rim seal fills the space between the internal

shell and the rim, it also allows the floating roof to rise and fall inside the tank. That is why, it constitutes one of the major components of the tank that the robot needs to inspect. There are two types of rim seals: primary and secondary [1]. The primary seals on one hand are available in three categories: mechanical, resilient and flexible wiper seals.

- **Mechanical Shoe:** This kind of seal incorporates a light-gauge metallic band which is made up of a series of sheet called shoes and attached together to form a ring.
- **Resilient Filled Seal:** Resilient Filled Seals are constituted by a core of open-cell foam covered by a coated fabric. The advantage of that type of seal is the ability of the used material to expand and contract, so there is permanent contact with the tank shell.
- **Flexible Wiper Seals:** The Flexible Wiper Seal is constituted from an annular blade of a flexible material fixed to a mounting bracket on the deck perimeter that spreads into the vapor space to touch the tank shell. There are two types of materials from which the blade is constituted. The first one involves elastomeric material and the common one is rubber. The second type consists of a foam core encapsulated in a coated fabric. The most used materials are Polyurethane on nylon fabric and polyurethane foam.

The secondary seals on the other hand allow to achieve a better evaporative losses control. They can be either flexible wiper seals or resilient filled seals.

## 2.3 Sensors for Robots in Tanks

The sensor choice has to respect constraints in oil tank which is a closed environment making the use of a GPS system impossible because the emitted signals cannot reach the robot inside the tank, as shown in Figure 2.11.

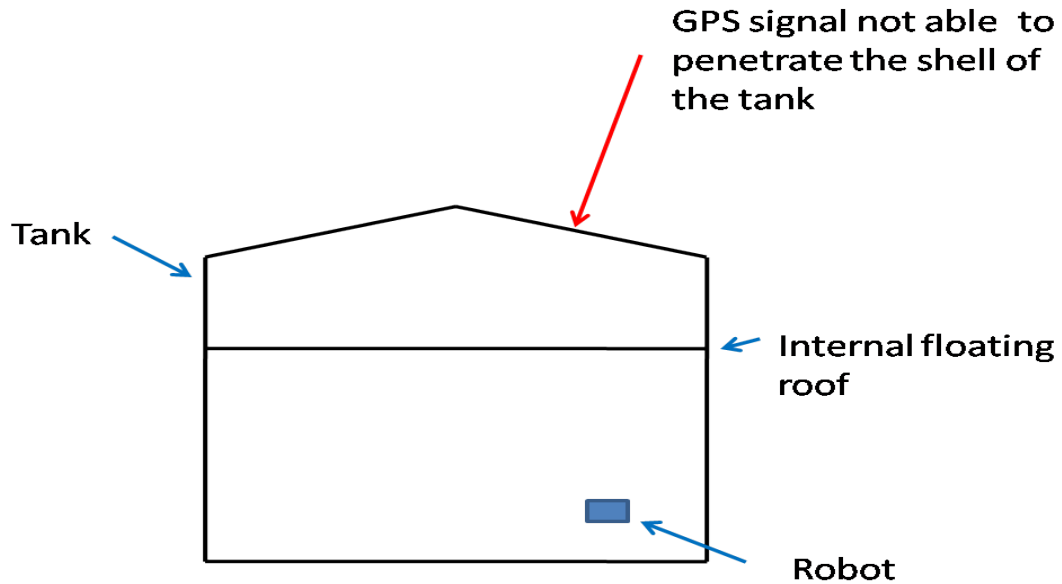


**Figure 2.11:** Problem of GPS Signal in Reaching the Robot

In fact, some of the types of tanks used in oil industry have a fixed and an internal roof. These are Internal floating Roof Tanks and Domed External Floating Roof Tanks. If the GPS signal is able to penetrate the first roof, it will be probably not able to penetrate the second roof. Likewise, an Inertial Navigation System cannot be used since it is usually integrated with a GPS and its size is big compared to the robot size. Side imaging Sonar is also big and cannot be fixed on small robots. The Underwater Acoustic Positioning System is supposed to be the best sensor since it uses the acoustic signals. But, as mentioned earlier, this system requires deploying transponders which may not be possible in this application. For our application, we select a proximity sensor that uses ultrasound, it sends a signal and when the latter bounces off of an object, an echo will be returned. The travel time of the echo will be recorded and by the knowledge of the velocity of the sound in the medium, the distance is calculated (see Figure 2.12).

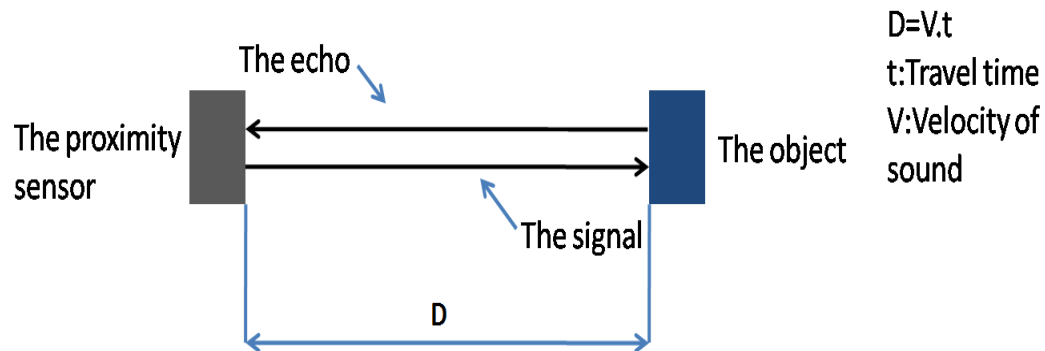


**Figure 2.12:** Proximity Sensor

Proximity sensors are suitable to this application since they are available in small size and they can work in hazardous environment if they are sealed, so the oil or the chemical could not damage the electronic part of the sensor. For rotation measurements, the best option is to use an electronic compass because it is small in size and it can compensate the effects of metallic walls and bottom. It also can calculate the angle of the robot when it is not in a horizontal plane for its ability of tilt compensation. The compass can be fixed in the enclosure where the electronic boards are fixed. This enclosure has to be sealed to prevent the entrance of oil or any chemicals. The sensor choice constitutes the first part to solve the localization problem and the second part deals with the choice of landmarks with respect to which the robot localizes itself. In fact, setting up the landmarks inside the tank is a difficult task. Then, it requires the facility to be emptied which results in a waste of time and substantial monetary expenditure. Mounting landmarks outside the tank is also not a good option for the fear that the signals will be not able to penetrate the shell of the tank. As a solution, it is necessary to exploit the circular geometry of tank as a structured environment and then localize the robot with respect to the wall. This idea was inspired from a previous work [4]. As a technical solution to determine the localization of the robot, a proximity sensor which uses ultrasonic signals and an electronic compass were chosen. The circular geometry plays the role of landmarks.

## 2.4 Conclusions

At the outset of this Chapter, an extensive literature review of sensors used for AUV was presented. This review enumerated sensors used for position and orientation measurements. They included Global Positioning System, Inertial Navigation System, Imaging Sonar, Visual-based Sensor, Underwater Acoustic System, Compass, Gyrocompass, Gyroscope and MEMS Gyroscope. This Chapter also discussed whether these sensors are appropriate to the use of robots for the inspection of AST. This Chapter then proceeded to present types of tanks used in the industry and the main parts to be inspected. It finished with giving the sensor choice.

The next Chapter presents how it is possible to localize the robot through the exploitation of the tank geometry and discusses how to decide on the number of sensors and their placement.

# Chapter 3

## Analytical Sensor Error Analysis

In many applications, to improve precision and performance, it is important to increase the number of sensors. For example, to localize an object with the Global Positioning System, four satellites are required. A GPS receiver uses the reception time of the signal to determine the distance to that satellite. Small errors in time calculation result in huge errors in location. Therefore to reduce uncertainty, we increase the number of measurements. Similarly, for this application, the number of ultrasonic sensors will highly affect the accuracy. This Chapter will be devoted to decide on the number of ultrasonic sensors as well as the angle between them based on error analysis. It is organized as follows: Section 3.1 briefly overviews a localization method from a previous work. Section 3.2 discusses simulation results of using respectively two, three and four sensors with different angles. It also summarizes advantages and drawbacks of each choice in terms of results accuracy. Finally, Section 3.3 concludes and discusses the contribution of this Chapter.

### 3.1 Previous Work

Abdulla *et al.* [4] used three distance sensors with relative angles equal to 120 degrees and an electronic compass to determine the orientation  $\phi$  defined as the angle between the x axis and the first sensor. Each distance sensor will output respectively  $d_1$ ,  $d_2$  and  $d_3$ . The first sensor is oriented with angle  $\theta_1$  equal to the angle  $\phi$ . The second sensor is oriented with  $\theta_2 = \phi + 120^\circ$  and the third sensor is oriented with  $\theta_3 = \phi + 240^\circ$ , as shown in Figure 3.1. The approach adopted is to exploit the tank geometry and to localize the robot with respect to the tank wall.

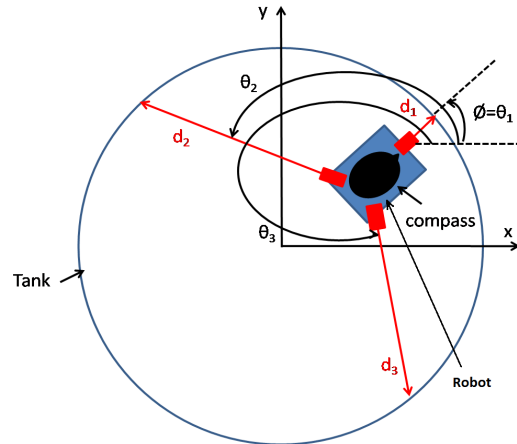


**Figure 3.1:** Robot in Oil Tank

In case we use only the measurements of the first sensor, the possible locations of the robot lie on the dotted arc of circle AB, as shown in Figure 3.2. This arc belongs to the circle centred at  $(-d_1 \cos \theta_1, -d_1 \sin \theta_1)$  with radius  $R$  which has the following equation:

$$(x + d_1 \cos \theta_1)^2 + (y + d_1 \sin \theta_1)^2 = R^2. \quad (3.1)$$

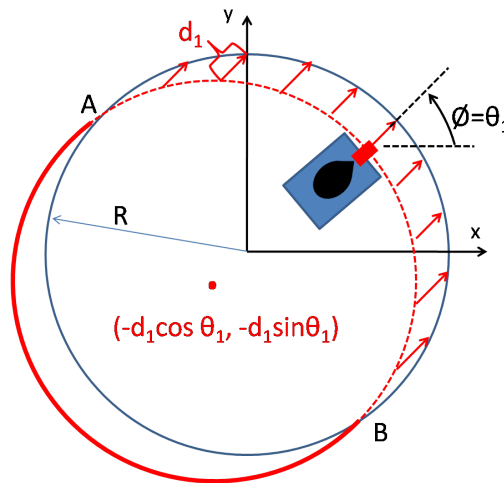


**Figure 3.2:** Localization with the First Sensor

The use of the second sensor indicates that the possible locations of the robot lie on the dotted arc of circle CD, as shown in Figure 3.3. This arc is a part of the circle centred

at  $(-d_2 \cos \theta_2, -d_2 \sin \theta_2)$  with radius  $R$  which has the following equation:

$$(x + d_2 \cos \theta_2)^2 + (y + d_2 \sin \theta_2)^2 = R^2. \quad (3.2)$$

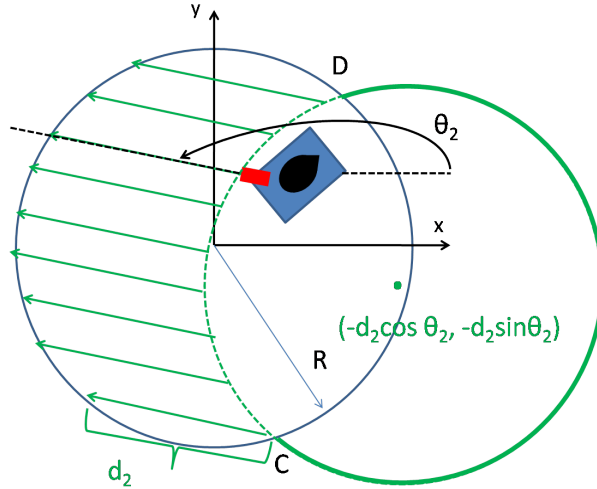


**Figure 3.3:** Localization with the Second Sensor

Similarly, based on the measurements of the third sensor, the possible locations of the robot lie on the dotted arc of circle EF, as shown in Figure 3.4. This arc is a part of the circle centred at  $(-d_3 \cos \theta_3, -d_3 \sin \theta_3)$  with radius  $R$  which has the following equation:

$$(x + d_3 \cos \theta_3)^2 + (y + d_3 \sin \theta_3)^2 = R^2. \quad (3.3)$$

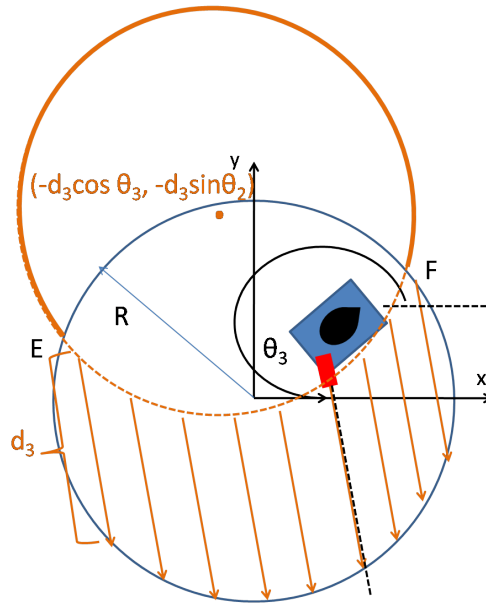


**Figure 3.4:** Localization with the Third Sensor

In order to determine the location of the robot within the tank, we have to solve the three equations (3.1), (3.2) and (3.3).

## 3.2 Error Analysis

Based on the previous work, we can ask the following questions:

- **Question 1:** How many sensors should we use?
- **Question 2:** What should be the relative angles between sensors?
- **Question 3:** What should be the measure of goodness?

In order to answer these questions, a whole study was done. We did the first study using only two sensors. In that case, two equations are sufficient to determine the position of the robot. But, two equations yield two possible positions. Adding a third sensor allows to get rid of this problem since the intersection of three circles gives only one point, this constitutes the second part of this study. The use of four sensors gives also only one

possible location, this constitutes the final part of the study. But, obtaining exact position of the robot is possible if and only if the measured distances are exact. However, sensors are subject to many sources of errors which translate in error in the position of the robot. How much is this error and how does it depend on the number of sensors as well as the relative angle between them, this is a major question that the following section will answer.

### 3.2.1 Localization with Two Sensors

In order to decide on the number of sensors and their placement, we adopted the error in the robot position as a measure of goodness. Suppose only two proximity sensors are used giving at some instance of time two measurements  $d_1$  and  $d_2$ . Equations (3.1) and (3.2) relate  $d_1$ ,  $d_2$  and the location position of the robot inside the tank  $(x, y)$ .

As stated previously, error in sensor readings will affect the accuracy of the robot position  $(x, y)$ , this is what we call error mapping. To explain more this idea, suppose for a point  $P$  with coordinates  $(x, y)$ , we have distance measurements:  $d_1 = d_1^* + e_1$  and  $d_2 = d_2^* + e_2$  where:

- $d_1^*$  corresponds to a nominal distance measurement given by sensor 1.
- $d_2^*$  corresponds to a nominal distance measurement given by sensor 2.
- $e_1$  corresponds to the error in sensor 1.
- $e_2$  corresponds to the error in sensor 2.

Let's call  $P^*$  the nominal position of the robot with coordinates  $(x^*, y^*)$  which correspond to nominal sensor measurements  $d_1^*$  and  $d_2^*$ .

When  $e_1 = 0$  and  $e_2 = 0$ ,  $d_1 = d_1^*$ ,  $d_2 = d_2^*$  and  $P(x, y) = P^*(x^*, y^*)$ . Therefore, the position of the robot is exact, as shown in Figure 3.5.

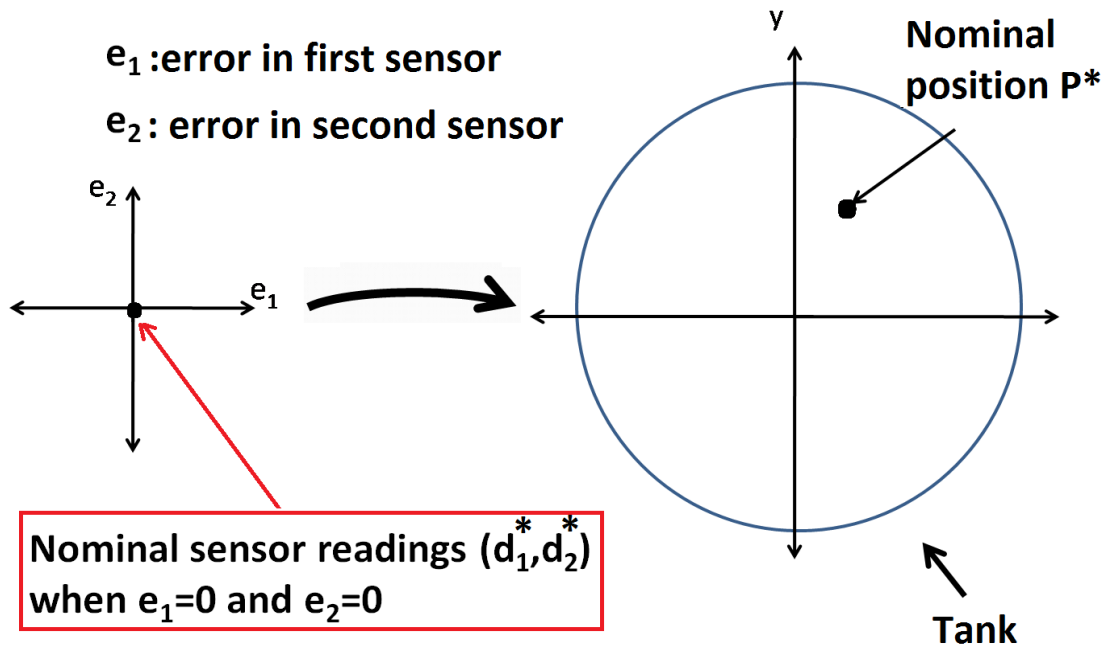


**Figure 3.5:** Error Mapping in Case of Zero Error in Sensors

However, sensors are liable to errors. For each combination of  $e_1$  and  $e_2$ , distance measurements deviate from the nominal distances. Therefore, the robot position  $P$  will deviate from the nominal position  $P^*$ . The robot positions resulting from each combination of  $e_1$  and  $e_2$  give an area called the error in the position, as shown in Figure 3.6.

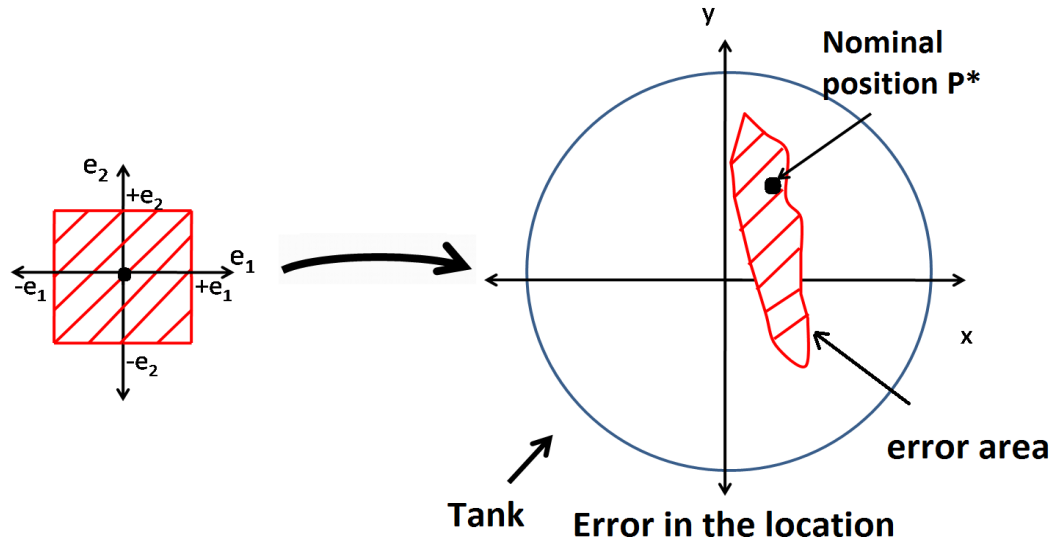


**Figure 3.6:** Error Mapping in Case of Error in Sensors

**Numerical Cases**

At this point, a possible measure of goodness is the area of the error. Figure 3.7 and Figure 3.8 show the error area corresponding to the nominal position  $P^*(10m, 10m)$  when the orientation  $\phi = 0$  and the relative angle  $\theta_2$  between the two sensors is equal to 180 degrees and 40 degrees respectively and under an error in each sensor  $e_1 = \pm 0.2m$  and  $e_2 = \pm 0.2m$ .

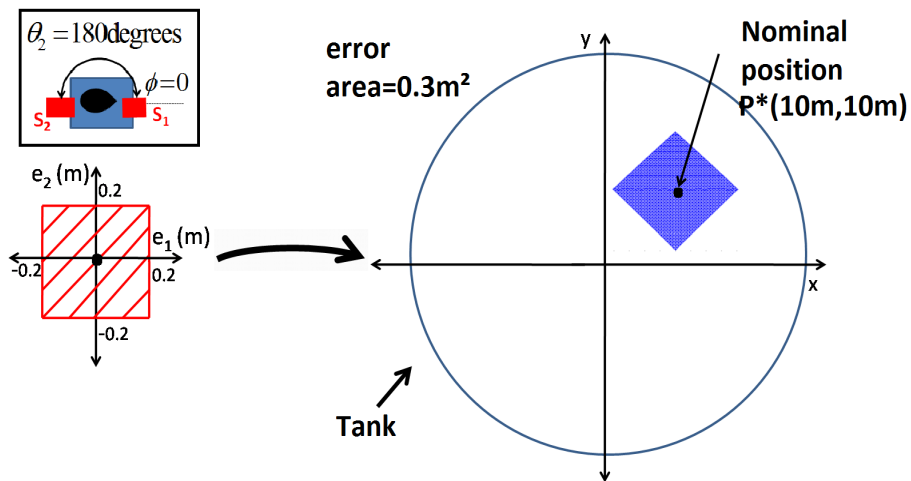


**Figure 3.7:** Error Mapping for the Case  $\theta_2 = 180$ degrees

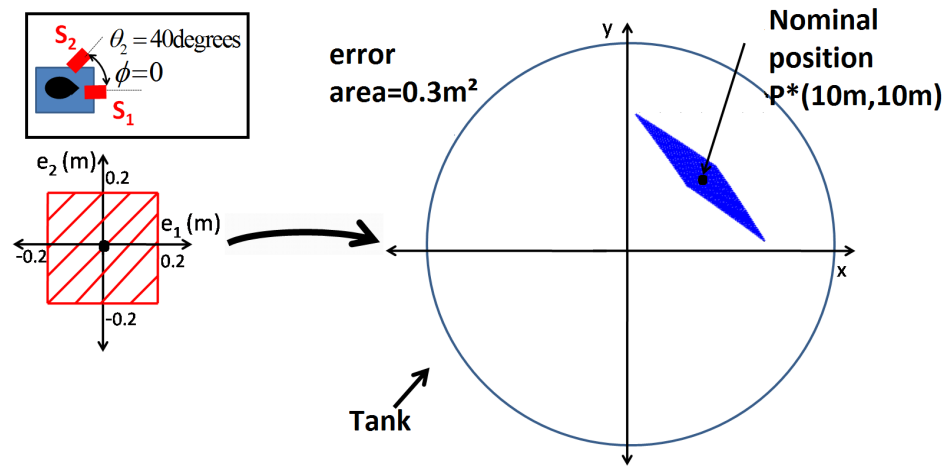


**Figure 3.8:** Error Mapping for the Case  $\theta_2 = 40^\circ$

These two simulations show that the error area is not well distributed around the nominal point. In fact, we have two different shapes that have the same area. Therefore, the error area is not a good measure of goodness. That is why, we adopt another measure of goodness which is the maximum error distance  $\rho$ . It is defined as the maximum distance from the nominal point to the furthest point in the error area, as shown in Figure 3.9.

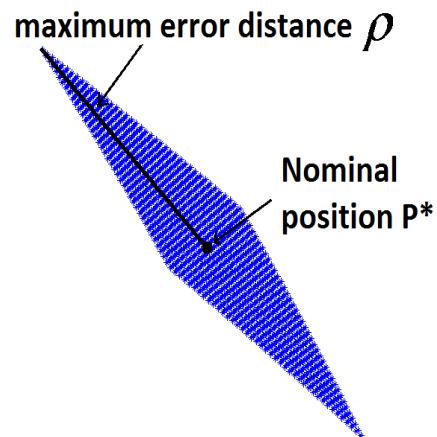


**Figure 3.9:** Maximum Error Distance  $\rho$

### A Graphically Solved Example

These are the steps to calculate the maximum error distance  $\rho$  graphically for an example where two sensors are used with a relative angle  $\theta_2$  equal to 180 degrees and  $\phi = 0$ , as shown in Figure 3.10.

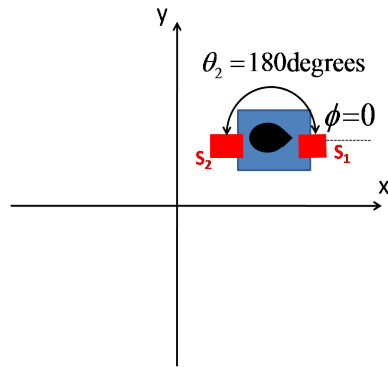


**Figure 3.10:** Sensors

1- Draw the contour of the tank (see Figure 3.11)

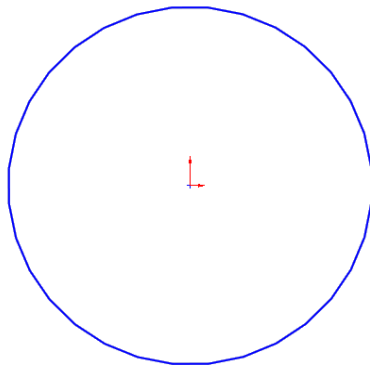


**Figure 3.11:** Tank Contour

2- Draw the nominal position and the distances read by each sensor (see Figure 3.12)

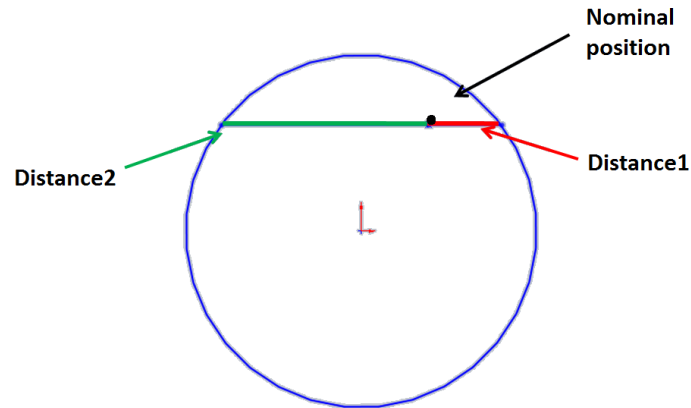


**Figure 3.12:** Nominal Point and Sensor Readings

3- Draw the nominal circles given by the two sensors (see Figure 3.13)

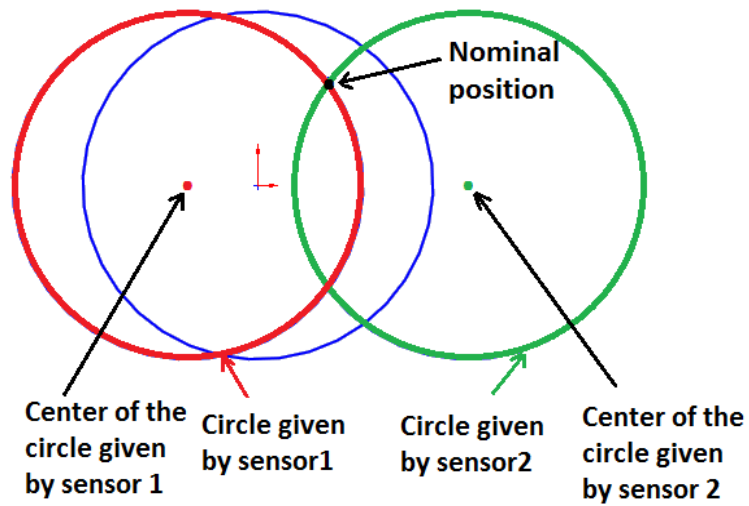


**Figure 3.13:** Nominal Circles of the Two Sensors

4- Draw the bands of circles resulting from the sensor error (see Figures 3.14)

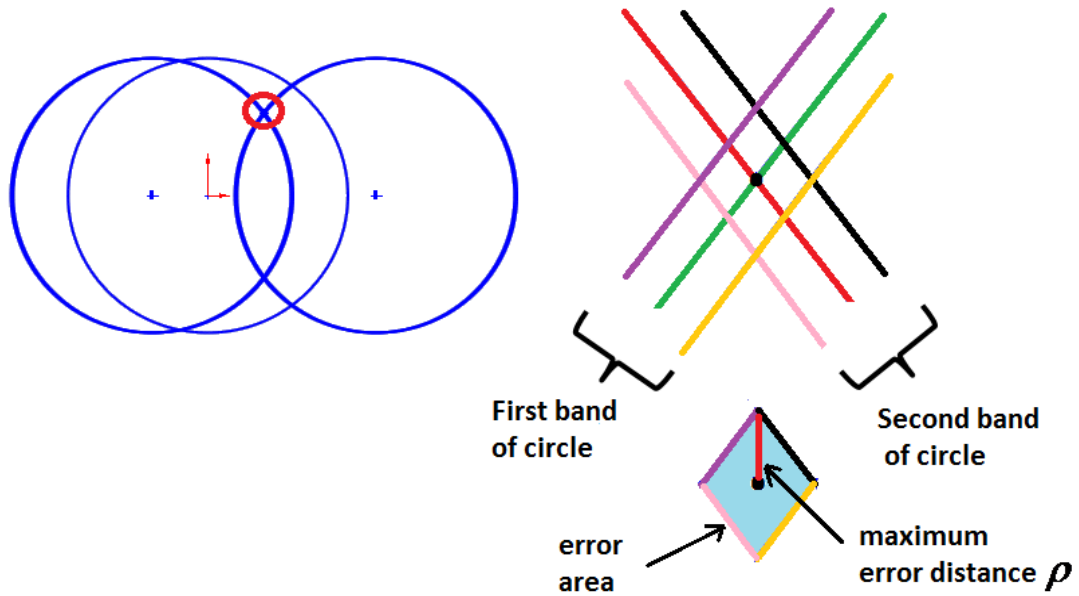


**Figure 3.14:** Position Error

### Simulation Case Study

Given  $d_1 = d_1^* \pm e_1$  and  $d_2 = d_2^* \pm e_2$  where  $e_1 = 0.2m$  and  $e_2 = 0.2m$ , we plot the maximum error distance  $\rho$  in the corresponding  $(x, y)$  position inside the tank. Figure 3.15 represents the maximum error distance  $\rho$  in the case of using two sensors with relative angle  $\theta_2$  equal to 180 degrees. The x axis corresponds to the  $x$  coordinate of a point in the tank and y axis corresponds to the  $y$  coordinate. The maximum error distance  $\rho$  is not distributed uniformly throughout the tank and it depends on the position  $P$ . For example, for  $P(10m, 15m)$ , the maximum error distance  $\rho$  is equal to  $1m$  and for  $P(0m, 3.5m)$ ,  $\rho$  is equal to  $7m$ .

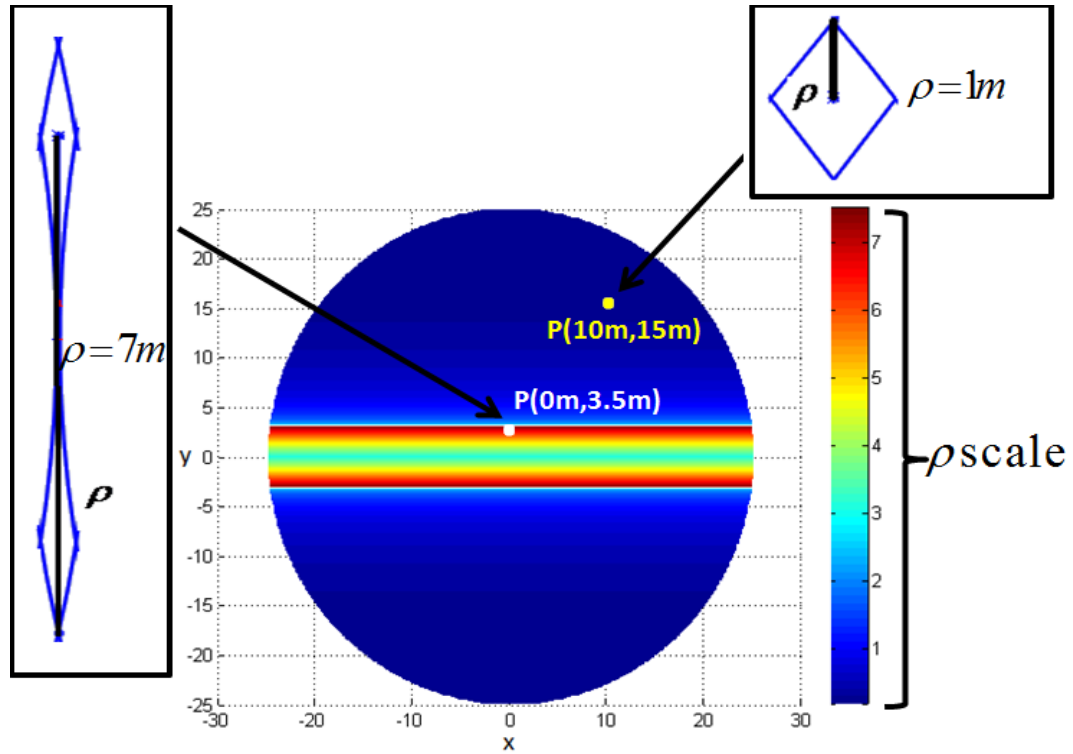


**Figure 3.15:** Simulation Case Study

For the remainder of this Chapter, we present the distribution of the maximum error distance  $\rho$  in the case of two, three and four sensors and for many sensor relative angles and robot orientations  $\phi$ .

### 3.2.1.1 First Case: $\phi = 0^\circ$

Figures included in Appendix A represent the maximum error distance  $\rho$  in the position for different values of the angle  $\theta_2$ . It turns out that with two sensors, the maximum error distance  $\rho$  can reach high values especially in the vicinity of the wall. Drawing the maximum error distance  $\rho$  also reveals that the use of two sensors can lead to two solutions. Two cases can occur: The first is that the two bands of circles indicating the possible locations of the robot by each sensor intersect in two error areas, one inside the tank and the other outside which means that only one physical solution exists (see Figure 3.16). On the contrary, the second case leads to two error areas both of them inside

the tank (see Figure 3.17). In this case, we have two solutions.

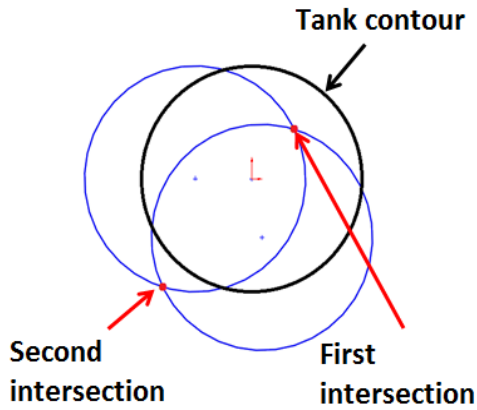


**Figure 3.16:** First Case

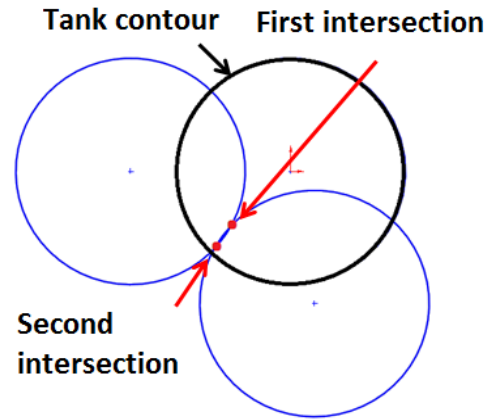


**Figure 3.17:** Second Case

When the relative angle between the two sensors is 180 degrees (see Figure A.5), the distribution of the maximum error distance  $\rho$  is symmetric relative to x and y axis. Even though, with that configuration, it is possible to have two solutions, this angle is still interesting because the right solution can be identified from the previous position of the robot.

### 3.2.1.2 Second Case: $\phi \neq 0^\circ$

Figure 3.18 and Figure 3.19 represent the case where we have the same relative angle 270 degrees between sensors but different orientations of the robot. Figure 3.18 corresponds to  $\phi = 0$  degrees and  $\theta_2 = 270$  degrees while Figure 3.19 corresponds to  $\phi = 40$  degrees and  $\theta_2 = 310$  degrees. It turns out that the maximum error distance  $\rho$  is sensitive to the orientation  $\phi$ . For example, for  $P(10,10)$ , the maximum error distance  $\rho$  increases with the increase of  $\phi$ . When  $\phi = 0$  degrees,  $\rho = 1m$ , and when  $\phi = 40$  degrees,  $\rho = 1.5m$ . Further simulations are included in Appendix B.

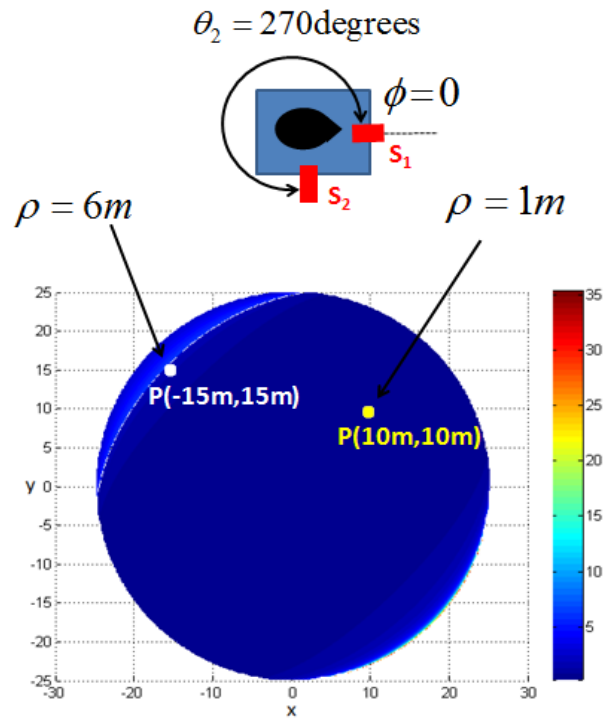


Figure 3.18: Two Sensors:  $\phi = 0^\circ$ ,  $\theta_2 = 270^\circ$

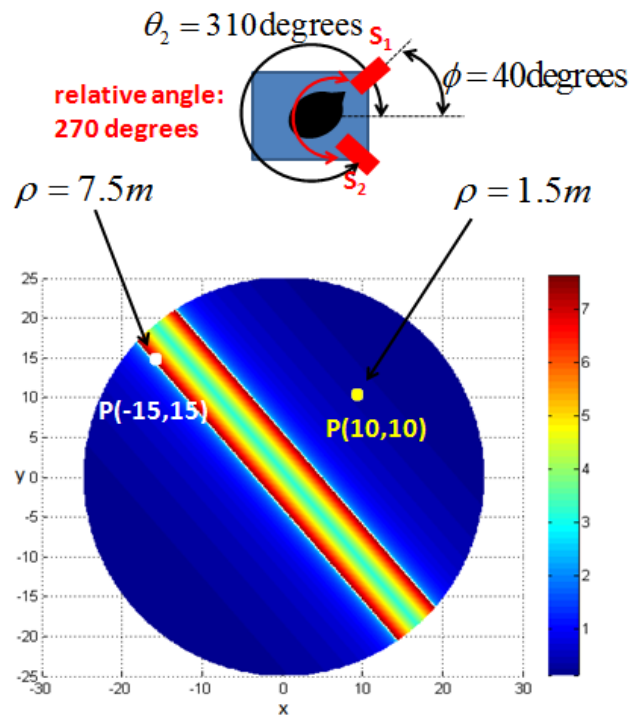
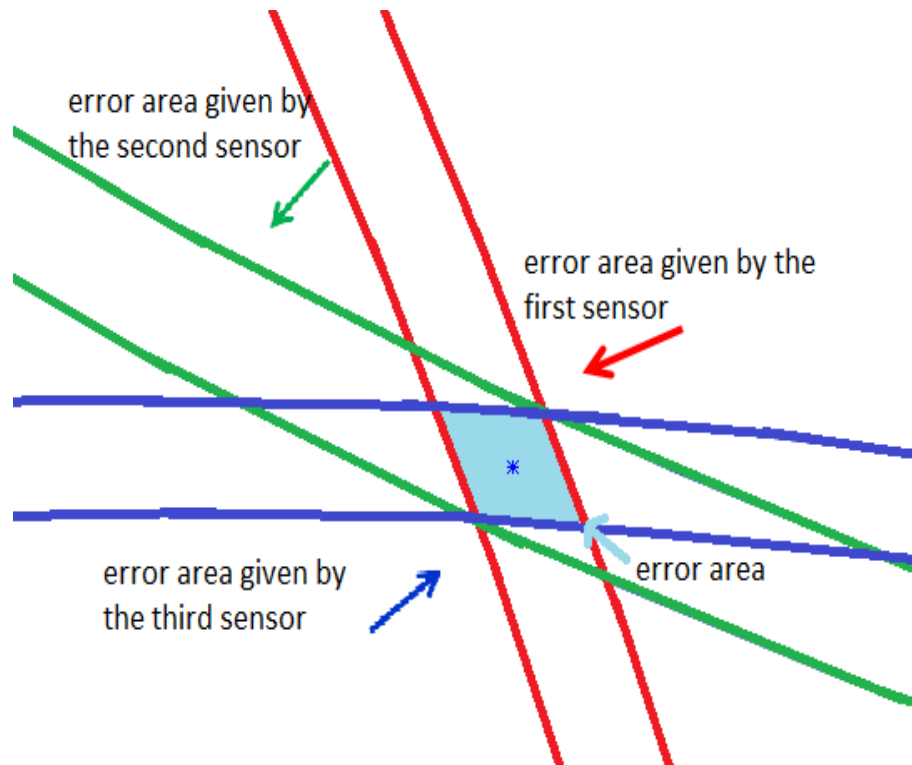


Figure 3.19: Two Sensors:  $\phi = 40^\circ$ ,  $\theta_2 = 310^\circ$

## 3.2.2 Localization with Three Sensors

### 3.2.2.1 First Case: $\phi = 0^\circ$

The use of three sensors is more advantageous than the use of two sensors. The main benefit is that with three sensors there exists only one solution and also the values of the maximum error distance  $\rho$  decrease dramatically compared with the case of two sensors. This is because the error area given by three sensors is the intersection of the error areas given by each two sensors, as shown in Figure 3.20.



**Figure 3.20:** Error Area Given by Three Sensors

When the relative angle between each two sensors is 90 degrees, the maximum error distance  $\rho$  reaches more than  $4m$ , as shown in Figure 3.21. But, with a relative angle equal to 120 degrees, it is only about  $3m$ , as shown in Figure 3.22. From the simulations, it appears that the maximum error distance  $\rho$  does not exceed  $1m$  in the majority of positions within the tank. This decrease results in more accurate position of the robot.

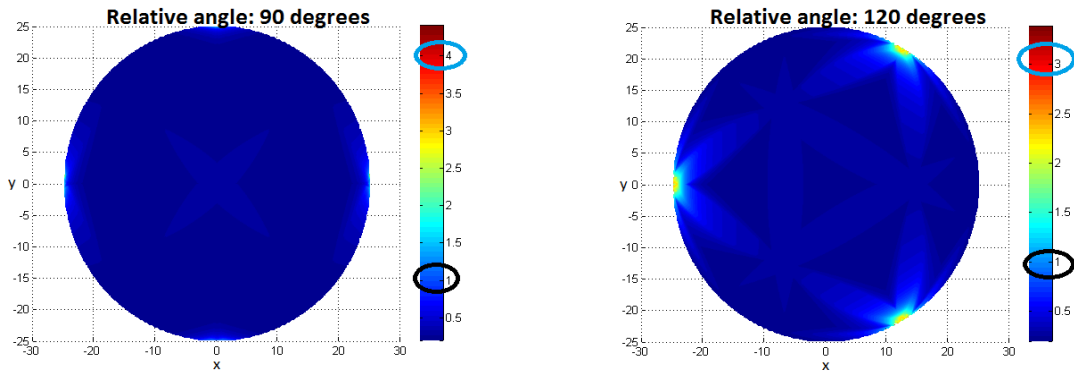


**Figure 3.21:** Three Sensors:  $\phi = 0^\circ$ ,  $\theta_2 = 90^\circ$ ,  $\theta_3 = 180^\circ$       **Figure 3.22:** Three Sensors:  $\phi = 0^\circ$ ,  $\theta_2 = 120^\circ$ ,  $\theta_3 = 240^\circ$

**3.2.2.2 Second Case:  $\phi \neq 0^\circ$**

Figure 3.23 and Figure 3.24 represent the distribution of the maximum error distance  $\rho$  when the relative angle between each two sensors is 90 degrees, while Figure 3.25 and Figure 3.26 represent the data when the relative angle is 120 degrees. In both cases, the maximum error distance  $\rho$  increases in the vicinity of the wall compared to the case of  $\phi = 0$ . It could reach more than 20m. This increase depends on the value of the angle  $\phi$ .

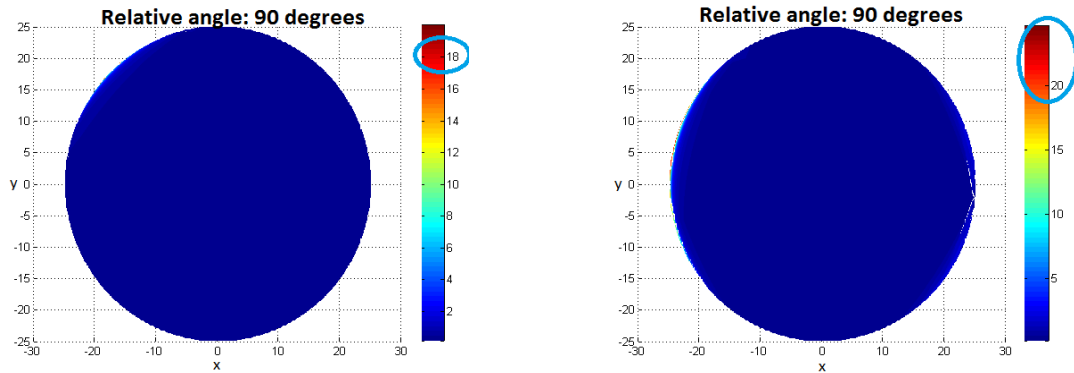


**Figure 3.23:** Three Sensors:  $\phi = 20^\circ$ ,  $\theta_2 = 110^\circ$ ,  $\theta_3 = 200^\circ$       **Figure 3.24:** Three Sensors:  $\phi = 40^\circ$ ,  $\theta_2 = 130^\circ$ ,  $\theta_3 = 220^\circ$

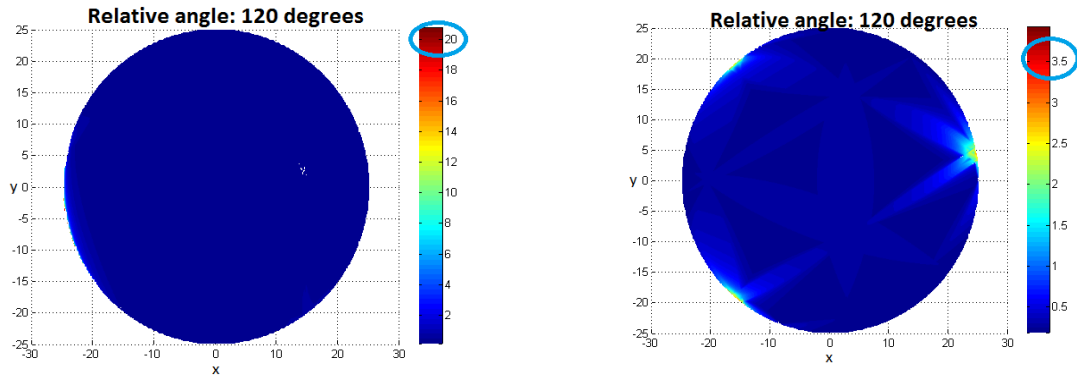


**Figure 3.25:** Three Sensors:  $\phi = 10^\circ$ ,  $\theta_2 = 130^\circ$ ,  $\theta_3 = 250^\circ$       **Figure 3.26:** Three Sensors:  $\phi = 70^\circ$ ,  $\theta_2 = 190^\circ$ ,  $\theta_3 = 310^\circ$

### 3.2.3 Localization with Four Sensors

#### 3.2.3.1 First Case: $\phi = 0^\circ$

The use of four sensors enables to obtain less value of the maximum error distance  $\rho$  compared to the case of two and three sensors. Its value is nearly constant in the majority of positions within the tank, as shown in Figure 3.27. It is about  $0.2m$ . The error area corresponding to four sensors is the intersection of all the error areas corresponding to each two sensors (see Figure 3.28). This is why the error area decreases and therefore the maximum error distance  $\rho$  decreases too. More importantly, it is interesting to use four sensors because it only gives one solution.

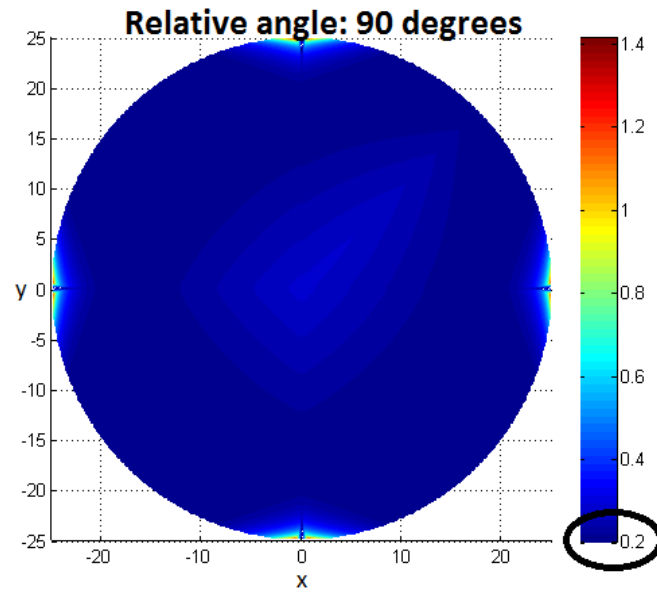


**Figure 3.27:** Four Sensors:  $\phi = 0^\circ$ ,  $\theta_2 = 90^\circ$ ,  $\theta_3 = 180^\circ$ ,  $\theta_4 = 270^\circ$

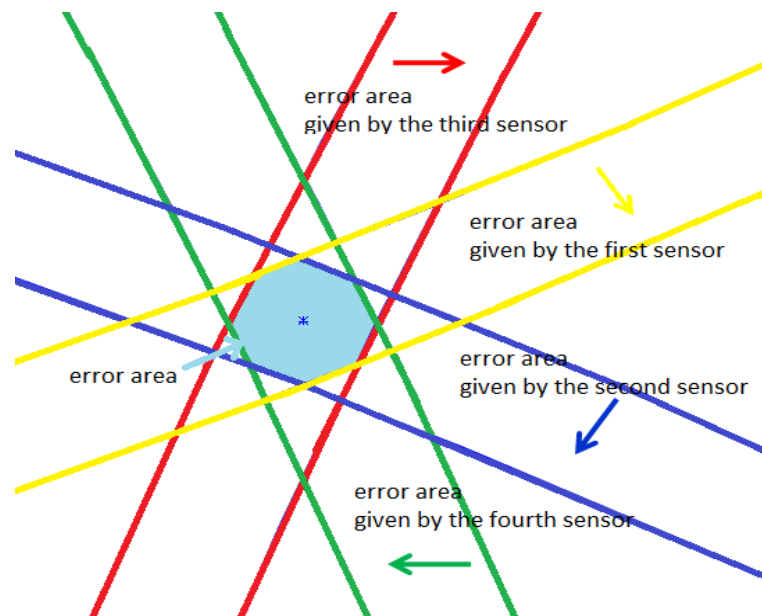


**Figure 3.28:** Error Area Given by Four Sensors

### 3.2.3.2 Second Case: $\phi \neq 0^\circ$

Similarly to the case of two sensors and three sensors, the simulations show that the maximum error distance  $\rho$  is sensitive to the angle  $\phi$ . But, this sensitivity is not very important. In fact, the maximum error distance  $\rho$  varies only in few positions that are near to the wall tank. The highest value of the maximum error distance  $\rho$  is around  $2m$  and is nearly the same for different values of  $\phi$ , as shown in Figures 3.29, 3.30 and 3.31.

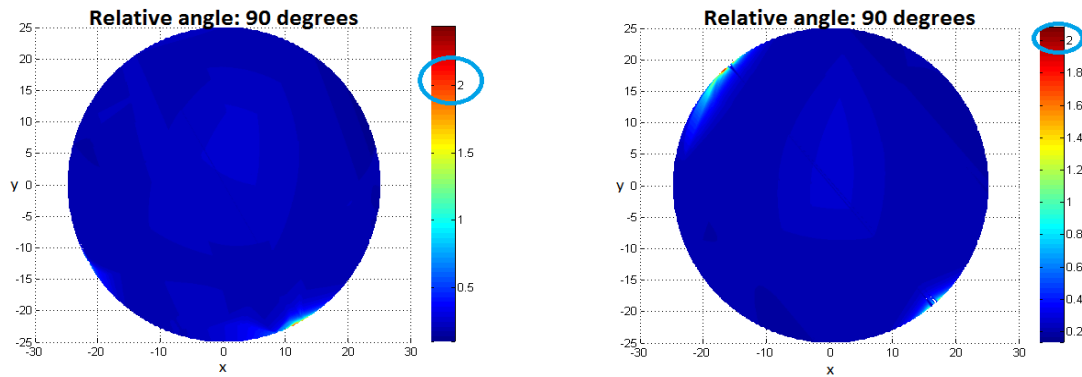


**Figure 3.29:** Four Sensors:  $\phi = 30^\circ$ ,  $\theta_2 = 120^\circ$ ,  $\theta_3 = 210^\circ$ ,  $\theta_4 = 300^\circ$       **Figure 3.30:** Four Sensors:  $\phi = 40^\circ$ ,  $\theta_2 = 130^\circ$ ,  $\theta_3 = 220^\circ$ ,  $\theta_4 = 310^\circ$

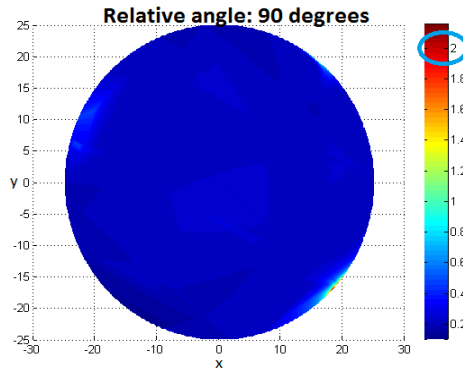


**Figure 3.31:** Four Sensors:  $\phi = 50^\circ$ ,  $\theta_2 = 140^\circ$ ,  $\theta_3 = 230^\circ$ ,  $\theta_4 = 320^\circ$

### 3.3 Conclusions

Through the error analysis, it turns out that as we increase the number of sensors as the maximum error distance  $\rho$  decreases and hence the error in determining the position of the robot diminishes. Many factors decide on the best number and placement of sensors. Mainly, the number of sensors is the principal factor that determines the number of obtained solutions. The use of three or four sensors yields always only one solution. But, the use of two sensors gives two solutions. This problem can be solved only if the relative angle is 180 degrees, otherwise, it is impossible to determine the exact location of the robot. The simulations also reveal that the relative angle between the sensors influences deeply on the accuracy of the results. As a conclusion, from this analysis, it appears that the best number of sensors is four with a relative angle equal to 90 degrees.

# Chapter 4

## Experiment and Results

Sensors constitute the heart of robotic applications by providing an interface to the real world. But, in real application, sensors are subject to some implementation issues that depend on the environment where the sensors are operating. This Chapter presents the conducted experiment to understand these issues and details the obtained results. The first section determines the objective of the experimental case studies. Section 2 describes the design of the experimental setup as well the chosen sensors. Likewise, Section 3 describes the experimental procedure. Section 4 presents the results. Finally, this Chapter ends with the conclusions.

### 4.1 Objective of the Experiment

The aim of this experiment is to test several issues related to the use of ultrasonic sensors, namely the reflection and the interference between signals. The interference occurs when two ultrasonic signals superimpose to give only one signal with different amplitude leading to wrong readings hence determining a false position of the robot. But, in real world and in some applications, it remains impossible to avoid this physical problem. Therefore, it is redundant to identify the sources of interference. Doing this, it is possible to enhance the performance of the robot by choosing the appropriate relative angle between the sensors. This experiment has two main parts. The first one shows that the relative angle between the sensors is an important factor that determines whether there is interference between the signals. The second part indicates that the interference depends on the location of the robot within the tank.

## 4.2 Design of the Experimental Setup

Figure 4.1 presents the experimental setup. It is composed from different parts which are listed in below.

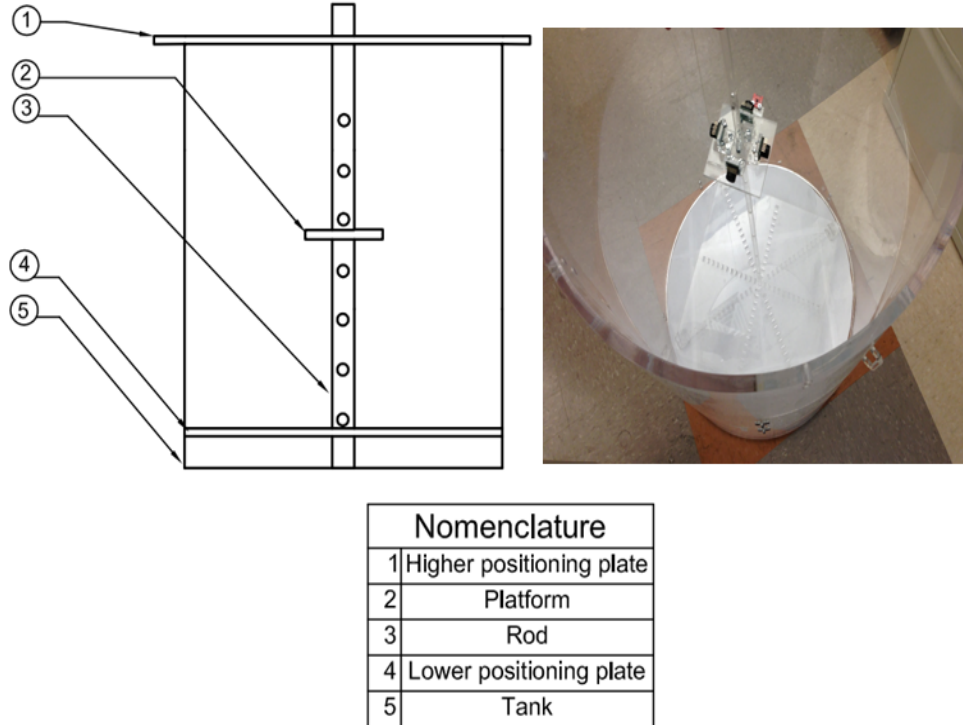


**Figure 4.1:** The Experimental Setup

### Tank:

For this experiment, a tank made up of plexiglass is used. It has a diameter of  $56\text{cm}$ . Normally, in the real application, tanks are constructed from metallic plates. But, because of the high reflection coefficient, a tank made up of plexiglass could be a good solution to conduct the experiment. By definition, the reflection coefficient [11] is defined as:

$$r = \frac{Z_1 - Z_2}{Z_1 + Z_2}, \quad (4.1)$$

where  $Z$  is the acoustic impedance which is equal respectively in plexiglass and air to:

$Z_{\text{plexiglass}} = 2.023\text{Pa.s/m}$  and  $Z_{\text{air}} = 428\text{Pa.s/m}$ . When the sound is propagated from air

to plexiglass, the absolute value of the reflection coefficient  $r$  is approximately equal to 1, so this shows that the plexiglass is a good reflector.

**Rod:**

A rod is attached to the platform. It maintains the platform horizontal to the bottom of the tank and contains many holes, as shown in Figure 4.2, so the platform can be fixed in different levels. Dimensions given in Figure 4.2 are in *mm*.

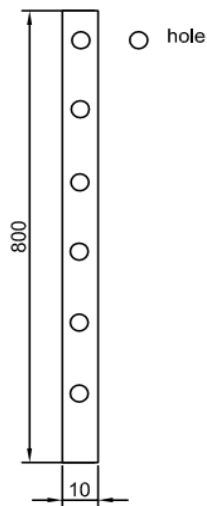


**Figure 4.2:** Rod

**Positining Plates:**

Two positioning plates are constructed to fix the platform at known positions. One is fixed in the bottom of the tank and the other is placed on the top to ensure the perpendicularity of the rod. Figure 4.3 shows the Higher Positioning Plate.

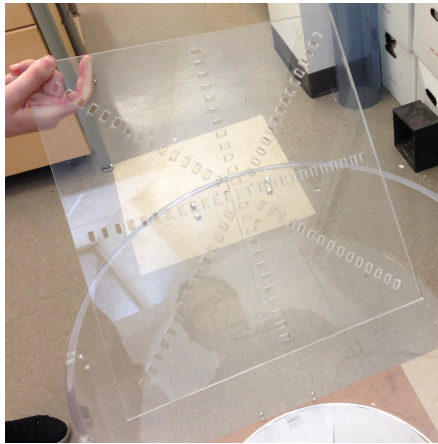


**Figure 4.3:** Higher Positioning Plate

**Platform:**

It is made of plexiglass and serves as a sensors holder, as shown in Figure 4.4 (dimensions are in *mm*). It contains a hole to fix the rod and many circular holes to fix the sensors. These sensors are four ultrasonic sensors and one compass. The ultrasonic sensors have to be able to range either simultaneously or in sequence, so the cross talk will be avoided. Besides, their beams have to be narrow enough to indicate a precise position because the tank is circular.

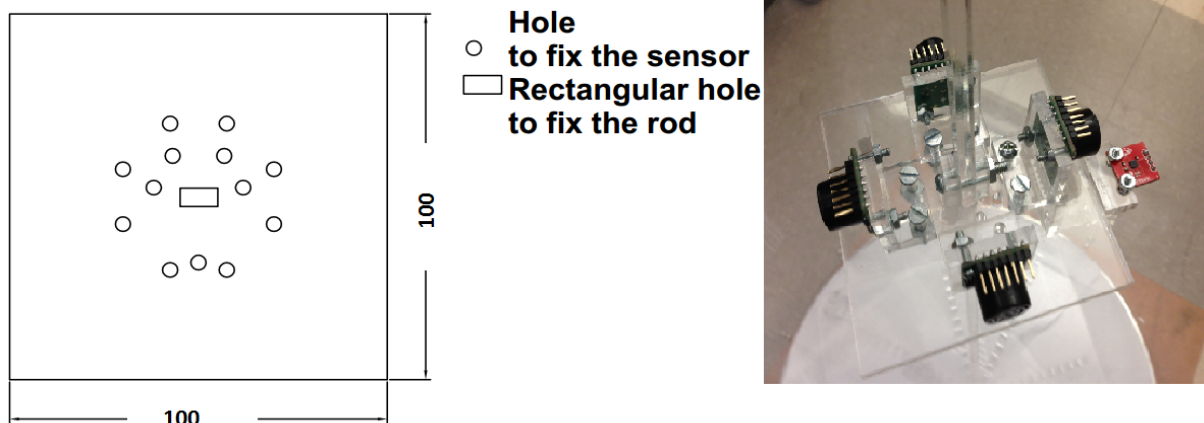


**Figure 4.4:** Platform

To interface the sensors to the computer, an Arduino Uno card is used. It is hard

wired to the sensors and connected to the computer through a USB cable, as shown in Figure 4.5.

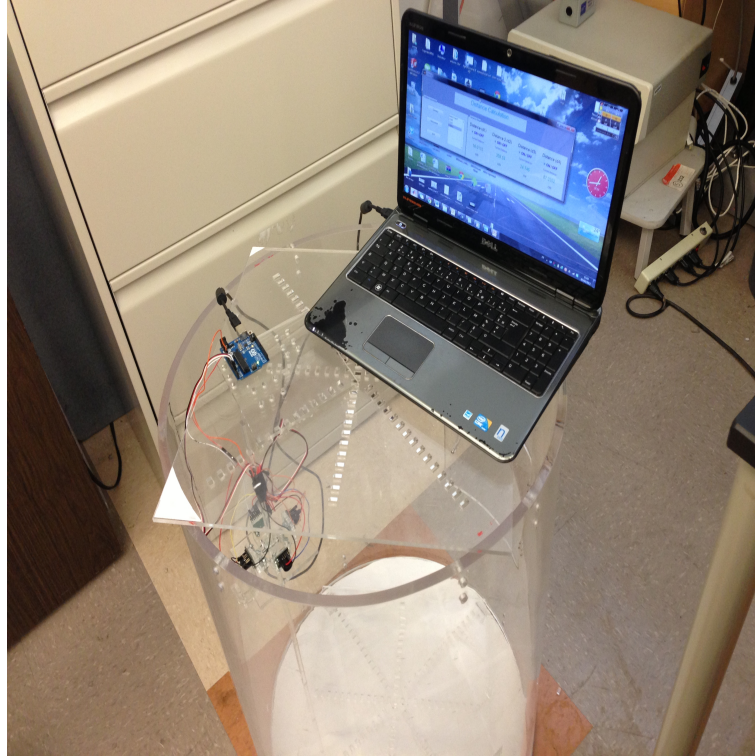


**Figure 4.5:** Electronic Board

### 4.3 Description of the Experiment

In real application, the robot inspects tanks filled with oil. But, this experiment is done in the air. The reason is because air is less viscous than oil. At  $T=20\text{ }^{\circ}\text{C}$  [12], air viscosity= $18.88\ 10^{-6}\text{ Pa}\cdot\text{s}$  and crude oil viscosity= $8.21\ 10^{-3}\text{ Pa}\cdot\text{s}$  [13]. Assuming that the propagation of the sound depends on the viscosity of the medium, the ultrasonic signals are less damped by air than oil. Therefore running the experiment in air enables us to obtain reliable results. Totally, we conducted two experiments.

- **Experiment 1:** The purpose of this experiment is to study the effect of the relative angles on the measurements. It consists in fixing the platform holding the sensors

at a known position which corresponds to the nominal distance  $d_1 = 428mm$ . Then, we visualize the distance measurement  $d_1$  of sensor 1 as a function of time  $t$ . The experiment is done firstly using three sensors and then four sensors. With three sensors, all the relative angles are equal to 120 degrees, as shown in Figure 4.6 and with four sensors, two relative angles are equal to 90 degrees, while the relative angle between sensor 1 and sensor 2 is 20 degrees and the relative angle between sensor 2 and sensor 3 is 160 degrees, as shown in Figure 4.7. The choice of these values of angles is to test the effect of small and big relative angles between sensors on the accuracy of the results.

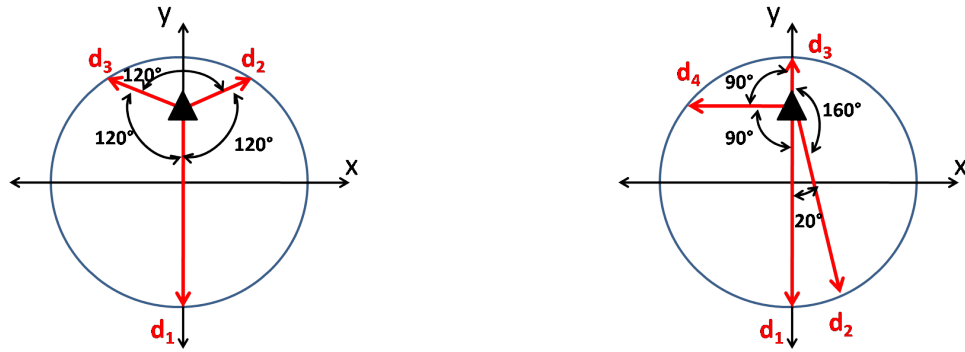


**Figure 4.6:** Experiment 1 with 3 Sensors    **Figure 4.7:** Experiment 1 with 4 Sensors

- **Experiment 2:** The purpose of this experiment is to study the effect of the position of the robot on the measurements. It consists in localizing the platform at different positions using firstly three sensors and then four sensors. At each position, the given data by each sensor are recorded. From these data, we compute the position and we verify whether it remains within the error area or not.

## 4.4 Results and Discussions

This section presents the results of each experiment. Both of the experiments prove that there exists interference but each one has its origins. The first and the second problem of

interference are related to experiments 1 and 2 respectively.

## 4.4.1 First Problem of Interference

### 4.4.1.1 Experiment with Three Sensors

Figure 4.8 presents the measured distance  $d_1$  by sensor 1. The x axis corresponds to the time and the y axis corresponds to the distance.

- For  $t \in [0s, 200s]$ , only sensor 1 is turned on.
- For  $t \in [200s, 600s]$ , both of sensors 1 and 2 are turned on.
- For  $t \in [600s, 800s]$ , only sensor 1 is turned on.

When  $t \in [0s, 200s]$ ,  $d_1$  fluctuates between  $423mm$  and  $438mm$  which are around the nominal distance  $d_1 = 428mm$ . When  $t \in [200s, 600s]$ , we observe that the curve shape does not undergo any change and sensor 1 continues outputting the same measurements. It turns out that sensor 1 is not affected by the sensor 2. As a result, 120 degrees is a good relative angle in case of using three sensors because it prevents the emitted signal by the sensor 1 to be interfered with sensors 2 signal. Curves corresponding to the use of sensor 1 and sensor 3 and to the use of three sensors are included in Appendix C and they are similar to Figure 4.8.

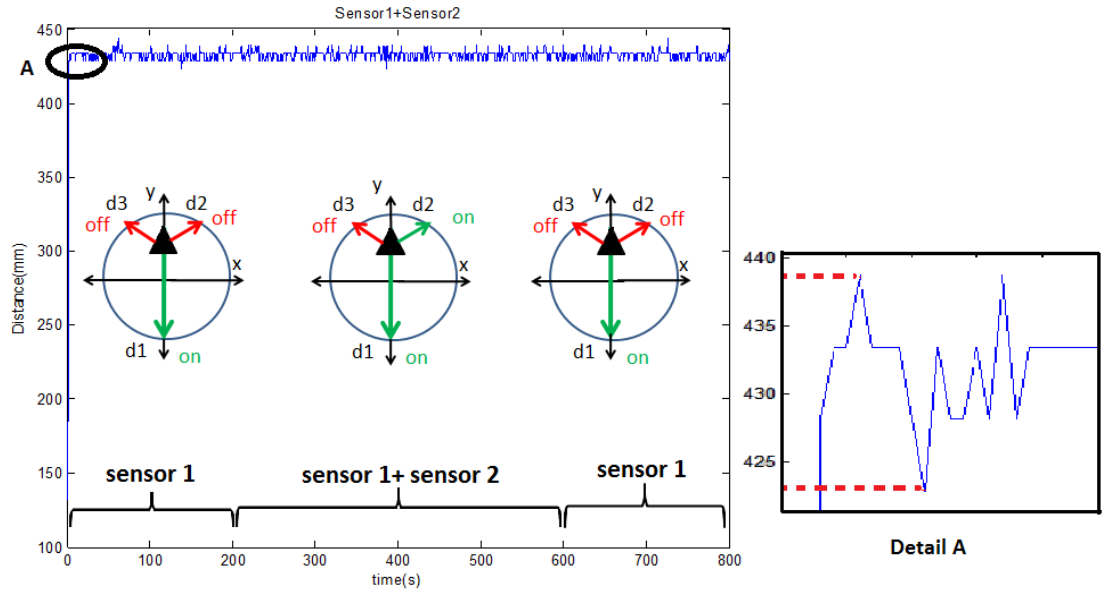


**Figure 4.8:** Experiment 1 with Three Sensors: Sensors 1 and 2

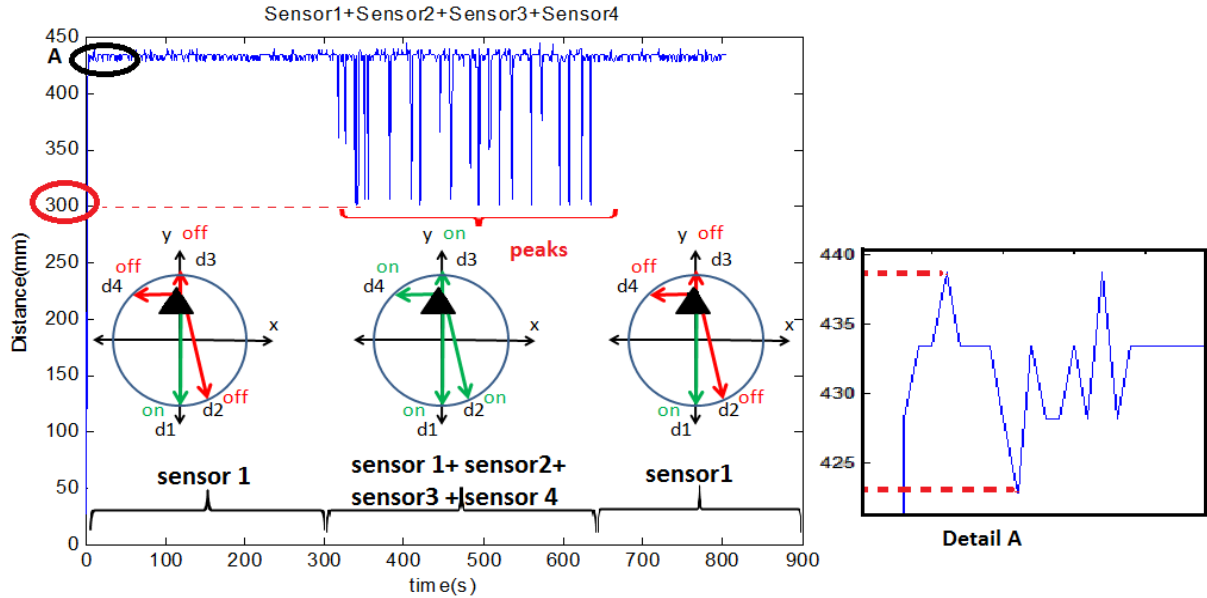
#### 4.4.1.2 Experiment with Four Sensors

Figure 4.9 presents the measured distance  $d_1$  by sensor 1 in the presence of three other sensors.

- For  $t \in [0s, 300s]$ , only sensor 1 is turned on.
- For  $t \in [300s, 650s]$ , all the sensors are turned on.
- For  $t \in [650s, 900s]$ , only sensor 1 is turned on.

When  $t \in [0s, 300s]$ ,  $d_1$  fluctuates between  $423mm$  and  $438mm$  which are around the nominal distance  $d_1 = 428mm$ . When  $t \in [300s, 650s]$ , we observe that the curve shape presents many peaks and sensor 1 gives very different measurements. It turns out that when sensor 2 is turned on, it disturbs the signal of sensor 1 which affects the distance measurements. The fluctuations are deeper and the first sensor gives  $d_1 = 300mm$  which is very far from  $d_1 = 428mm$ . This is due to the relative angle between sensor 1 and sensor 2 which is equal to 20 degrees. As a result, in the case of four sensors, small angles are

sources of interference which cause wrong measurements. Further curves that correspond to the case of four sensors are included in Appendix D.



**Figure 4.9:** Experiment 1 with Four Sensors: Sensors 1, 2, 3 and 4

#### 4.4.2 Second Problem of Interference

The second experiment consists in positioning the platform in many known positions and reading the distances given by each sensor. From the measurements, we calculate the position and we verify if it is inside the error margin resulting from error in sensors. Similar to the previous experiment, three sensors are used and then four sensors.

Tables (4.1) and (4.2) give the values of the nominal distances, the measured distances corresponding to different positions and angles  $\phi$ . The first table presents the measured data when using three sensors with a relative angle equal to 120 degrees. The second table presents the measured data when using four sensors with a relative angle equal to 90 degrees.

Table 4.1: Experiment 2 with Three Sensors

Angle $\phi$	Position		Nominal Distances			Measured Distances			Within Error Margin Yes/No
	$x(cm)$	$y(cm)$	$d1(cm)$	$d2(cm)$	$d3(cm)$	$d1(cm)$	$d2(cm)$	$d3(cm)$	
-90 deg	0	0	24.888	24.888	24.888	21.83	22.55	21.83	Yes
-90 deg	0	1.5	26.388	24.081	24.081	26.008	24.74	23.28	Yes
-90 deg	0	-4.5	20.388	26.921	26.921	19.645	not stable	not stable	No
0 deg	1.5	0	23.408	25.824	25.824	21.83	24.74	24.74	Yes
0 deg	4.5	0	20.408	26.915	26.915	18.92	not stable	not stable	No

Table 4.2: Experiment 2 with Four Sensors

Angle $\phi$	Position		Nominal Distances				Measured Distances				Within Error Margin Yes/No	
	$x(cm)$	$y(cm)$	$d1(cm)$	$d2(cm)$	$d3(cm)$	$d4(cm)$	$d1(cm)$	$d2(cm)$	$d3(cm)$	$d4(cm)$		
-90 deg	0	0	23.188	23.188	23.188	23.188	22.555	21.83	22.555	21.83	21.83	Yes
-90 deg	0	-1.5	21.688	23.148	24.688	23.148	21.3	22.555	25.3765	21.83	21.83	Yes
0 deg	6	0	17.188	22.543	29.835	22.543	17.46	not stable	29.835	not stable	not stable	No
0 deg	1.5	0	21.688	22.42	24.688	22.42	21.83	22.555	23.285	21.83	21.83	Yes
45 deg	-3.181	-3.181	27.688	22.827	18.688	22.827	27.65	not stable	18.92	not stable	not stable	No

Depending on the position of the platform, the measurements could be stable or unstable.

- **Stable Measurements:**

The measurements are stable if they do not deviate much from the nominal distances.

- **Unstable Measurements:**

The measurements are unstable if the deviation from the nominal distances is big.

The following figures show results of the experiment giving stable and unstable values in the case of three and four sensors.

### Experiment with Three Sensors

In the position shown in Figure 4.10, the nominal values of each distance are:  $d_1 = 24.888cm$ ,  $d_2 = 24.888cm$  and  $d_3 = 24.888cm$ . Figure 4.11 shows the experimental measurements of each sensor and it turns out that all the values are stable.

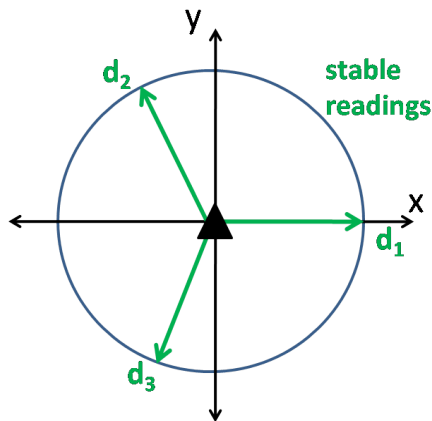


**Figure 4.10:** Experiment 2 with Three Sensors Giving Stable Measurements

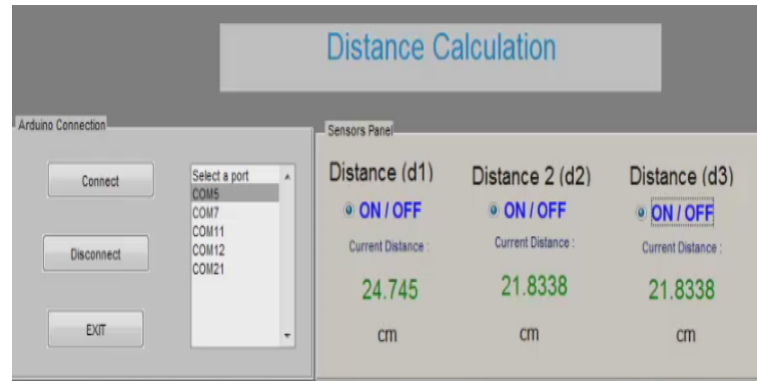


**Figure 4.11:** Matlab Window Showing Stable Measurements with Three Sensors

In the position shown in Figure 4.12, the nominal values of each distance are:  $d_1 = 21.409\text{cm}$ ,  $d_2 = 22.37\text{cm}$  and  $d_3 = 25.22\text{cm}$ . Figure 4.13 shows the experimental measurements of each sensor and it turns out that only the distance  $d_1$  is stable whilst  $d_2$  and  $d_3$  are unstable.

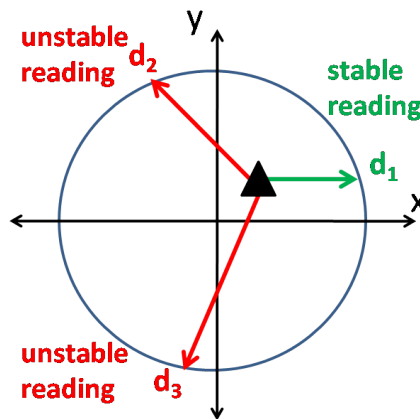


**Figure 4.12:** Experiment 2 with Three Sensors Giving Unstable Measurements



**Figure 4.13:** Matlab Window Showing Unstable Measurements with Three Sensors

### Experiment with Four Sensors

In the position shown in Figure 4.14, the nominal values of each distance are:  $d_1 = 21.4097\text{cm}$ ,  $d_2 = 21.445\text{cm}$ ,  $d_3 = 24.406\text{cm}$  and  $d_4 = 24.388\text{cm}$ . Figure 4.15 shows the experimental measurements of each sensor and it turns out that all the values are stable.

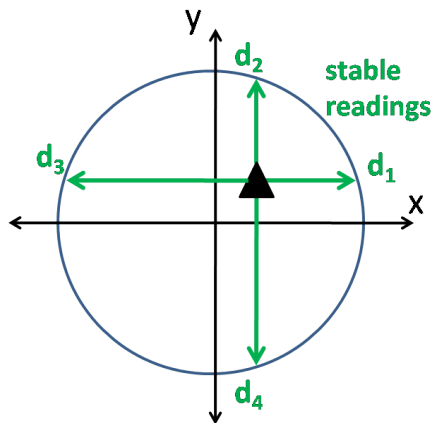


**Figure 4.14:** Experiment 2 with Four Sensors Giving Stable Measurements

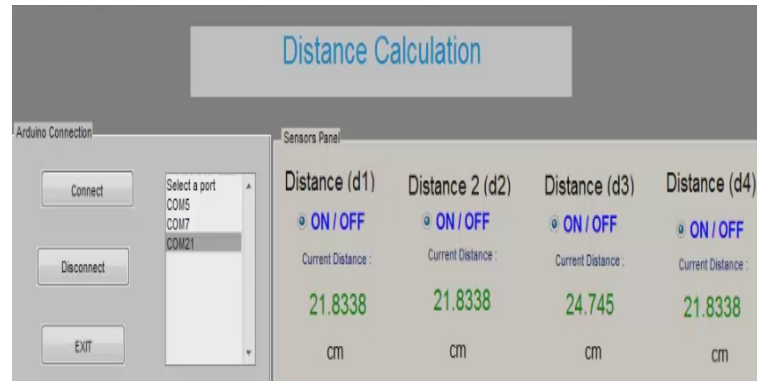


**Figure 4.15:** Matlab Window Showing Stable Measurements with Four Sensors

In the position shown in Figure 4.16, the nominal values of each distance are:  $d_1 = 15.4\text{cm}$ ,  $d_2 = 23.4077\text{cm}$ ,  $d_3 = 30.508\text{cm}$  and  $d_4 = 20.443\text{cm}$ . Figure 4.17 shows the experimental measurements of each sensor and it turns out that distances  $d_1$  and  $d_3$  are stable whilst  $d_2$  and  $d_4$  are unstable.

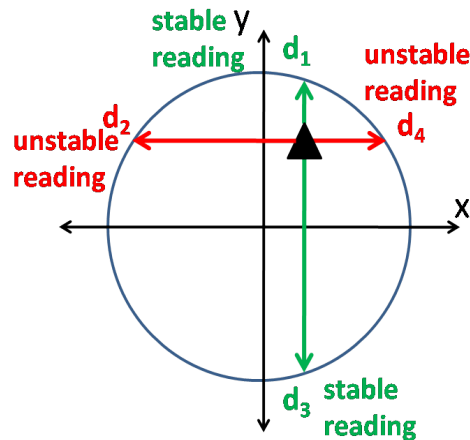


**Figure 4.16:** Experiment 2 with Four Sensors Giving Unstable Measurements

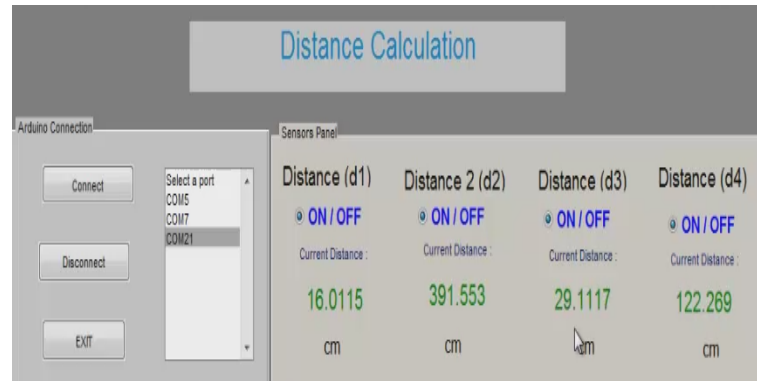


**Figure 4.17:** Matlab Window Showing Unstable Measurements with Four Sensors

In the case of stable values, the position of the platform is within the error margin called also error area, but when the sensor gives unstable value, the position is outside this area. This is validated graphically. The first step of the validation process is to plot the error margin. Taking into consideration that sensors are not perfectly accurate, if these nominal distances are measured with the sensors, they will give a position that is contained in a specific area around the nominal position. This area is determined from the intersection of the four bands of circles under an error of each sensor equal to  $\pm 1inch$ , as shown in Figure 4.18.

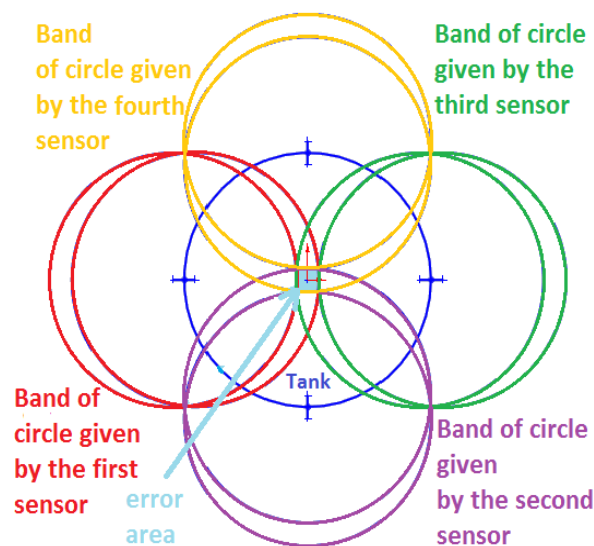


**Figure 4.18:** Error Area

The second step is to calculate the position of the platform from the measured distances. Each sensor indicates that the position is defined with an arc of circle, as shown in Figure 4.19.

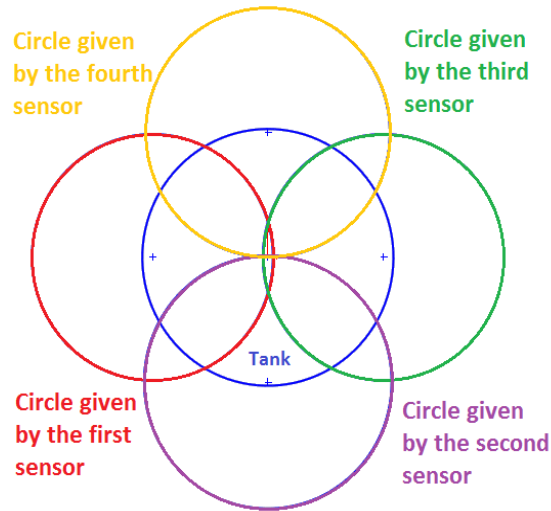


**Figure 4.19:** Intersection of the Circles

As the sensors are not accurate, the circles do not intersect in one point, but they will give an area, as shown in Figure 4.20.

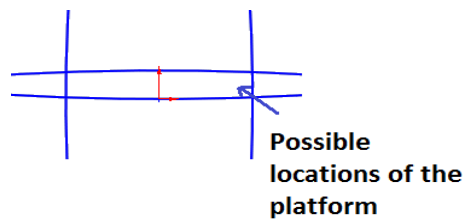


**Figure 4.20:** Possible Locations of the Platform

In that case, the position is estimated to the centroid of that area. Finally, we verify if the centroid is contained within the error margin determined in the first step.

The phenomenon that causes instability of measurements is the interference between the signals. When the platform is positioned around the center of the tank, as shown in

Figure 4.21, this problem does not arise. In that case, the signal emitted by each sensor is reflected by the wall with small reflection angle. But, when the platform is moved, some of the sensors give unstable values. These are the sensors whose emitted signals are reflected by the wall with big angle.

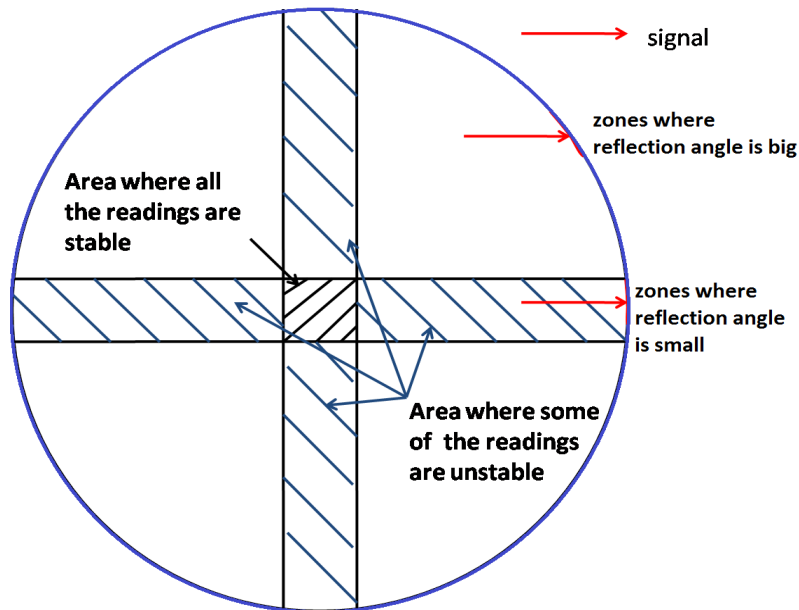


**Figure 4.21:** Stability and Instability Areas

In these positions where we have instability of measurements, the signal interferes with other signals. This is the result of the reflection angle that causes the signal to be reflected. Actually, the reflection exists whatever the reflection angle is due to the material of the tank which is a good reflector. But, when this angle is large, the reflected signal could reach another side in the tank before being attenuated, as shown in Figure 4.22. It continues to be reflected until it interferes with other signals. Therefore, it causes a wrong value of the distance. This problem does not manifest when the reflection angle is small.

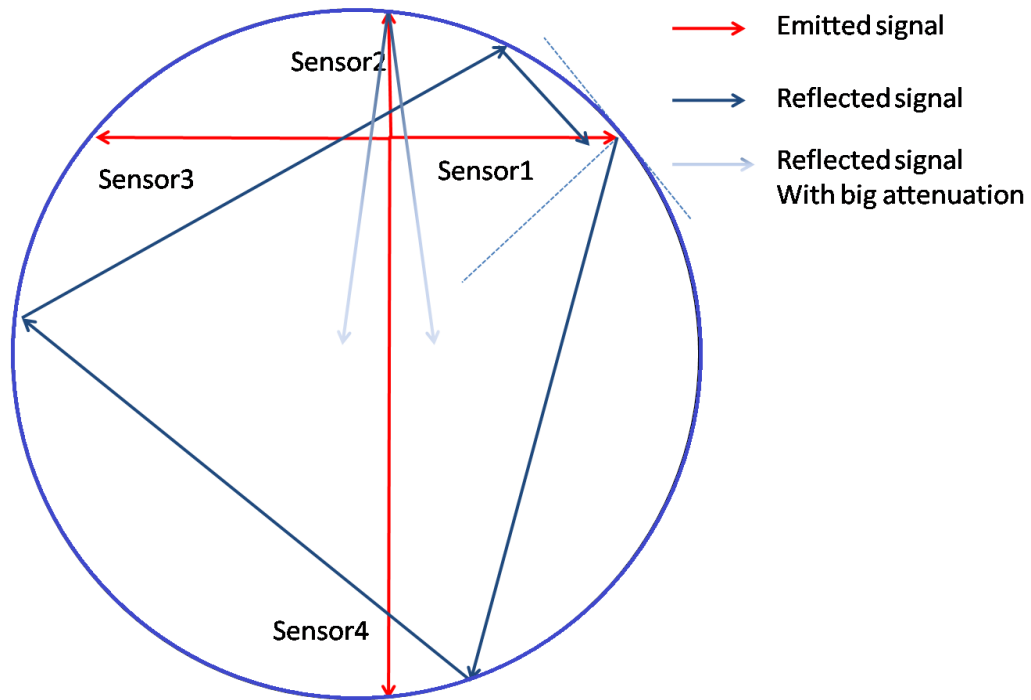


Figure 4.22: Signal Reflection

## 4.5 Conclusions

Through this experimental study, the implementation issues of ultrasonic sensors were investigated. The main problem is the interference between signals that yields wrong measurements. The two main factors behind this problem are the relative angle between sensors and the position of the robot within the tank. This experiment could be done every time we have a similar application to verify that the relative angle does not affect the measurements before implementation. But this experimental study is extreme because the tank used for this experiment is small with a diameter  $56\text{cm}$  while in the real application tanks reach a diameter of  $50\text{m}$ .

# Chapter 5

## Conclusions and Future Works

The inspection of oil tanks is an imperative task that aims to look for defects and cracks. Therefore, the safety of the facility is ensured by repairing these failures. The traditional methods could be a solution if the defect is from outside. But, in case the defect is inside the tank, the traditional methods are limited. The use of robot is an alternative solution that accomplishes the inspection task in less time and with optimal conditions. But, the use of robot requires ensuring the navigation within the tank. Simultaneous Localization and Mapping (SLAM) is a key to ensure that goal. It deals with the problem of building a map of an unknown environment by a robot while simultaneously using this map to navigate in the environment. SLAM is constituted of two parts, localization and mapping. In this thesis, we addressed the localization part of this problem.

To be able to localize the robot, it is essential to choose appropriate landmarks or references and to use sensors that can work in explosive liquids within metallic tanks. To that end, since tank is structured, we opted for its geometry as a landmark. To choose proper sensors, we reviewed the sensors used for Autonomous Underwater Vehicle in details since it is operating in unconstrained environment. To summarize, these sensors included Global Positioning System, Inertial Navigation System, Imaging Sonar, Visual-based Sensor, Underwater Acoustic System, Compass, Gyrocompass, Gyroscope and MEMS Gyroscope. We proceeded then to discuss whether each one is useful in our application. At the outset of this part, we chose proximity sensors that use ultrasonic signals to determine the position of the robot and a magnetic compass to determine the orientation.

The sensor choice alone is not sufficient to ensure the localization of the robot with high performance. Therefore, this thesis presented an error analysis study that aims to determine the best number of ultrasonic sensors and the relative angle yielding the least error. The error analysis study was based on choosing a measure of goodness to characterize the error in the robot location. The best choice was to opt for the maximum error distance  $\rho$  to decide on the optimal number of sensors and their placements. This study was done using respectively two, three and four sensors with different relative angles and different orientations  $\phi$ . Several simulation results of the error analysis were presented and they revealed that the error mapping in computing position is sensitive to the number of sensors, sensor relative placement, absolute robot location and robot orientation. At the end, we concluded that four sensors with relative angle equal to 90 degrees is the best configuration that gives the most exact position of the robot.

Finally, the problems that arise from the implementation were addressed through several experiments. The reflection and the interference between signals are the main issues related to the use of ultrasonic signals. This thesis presented two main sources of interference which are the small relative angles between sensors and the robot position within the tank. The experimental study enables to choose the best relative angles between sensors that give most accurate robot position. It proves that 90 degrees is a good relative angle that prevents sensors signals to be interfered with each other.

This thesis has only studied the localization problem, but the vision of this work is ambitious. Future work will focus on studying both the mapping and the localization. An experiment with a real robot and in a bigger tank could be done to provide more reliable results. Once this is done, an important step in the field of oil tank inspection will be achieved.

# Appendix A

## Localization with Two Sensors: $\phi = 0^\circ$

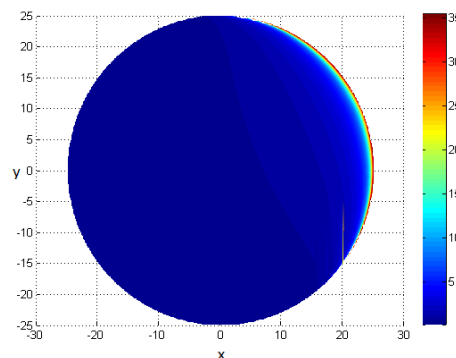
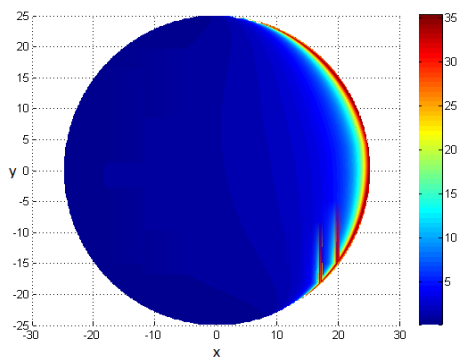


**Figure A.1:** Two Sensors:  $\phi = 0^\circ$ ,  $\theta_2 = 20^\circ$  **Figure A.2:** Two Sensors:  $\phi = 0^\circ$ ,  $\theta_2 = 45^\circ$

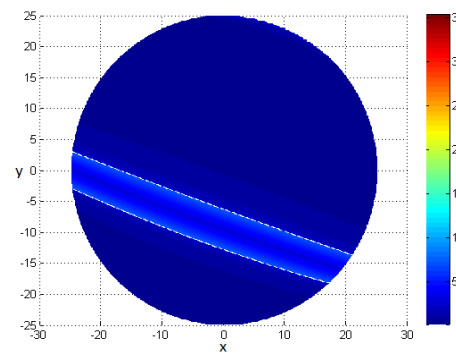
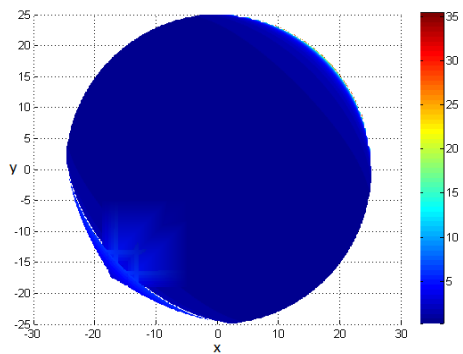


**Figure A.3:** Two Sensors:  $\phi = 0^\circ$ ,  $\theta_2 = 90^\circ$  **Figure A.4:** Two Sensors:  $\phi = 0^\circ$ ,  $\theta_2 = 140^\circ$

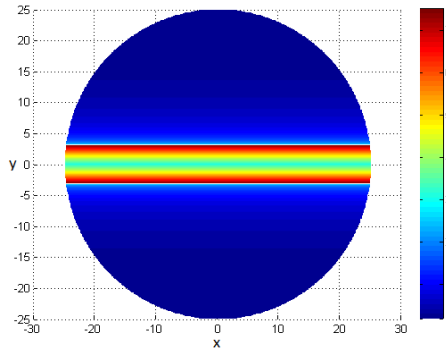


**Figure A.5:** Two Sensors:  $\phi = 0^\circ$ ,  $\theta_2 = 180^\circ$

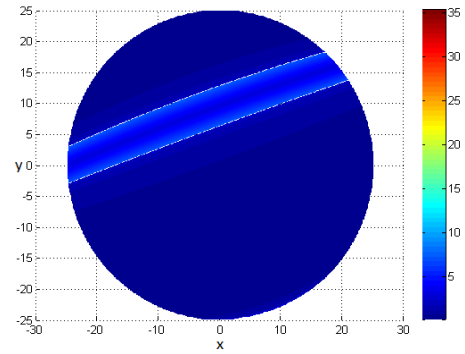


**Figure A.6:** Two Sensors:  $\phi = 0^\circ$ ,  $\theta_2 = 220^\circ$

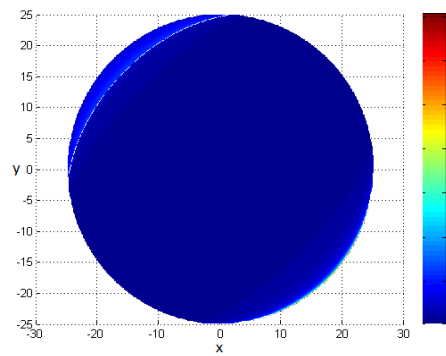


**Figure A.7:** Two Sensors:  $\phi = 0^\circ$ ,  $\theta_2 = 270^\circ$

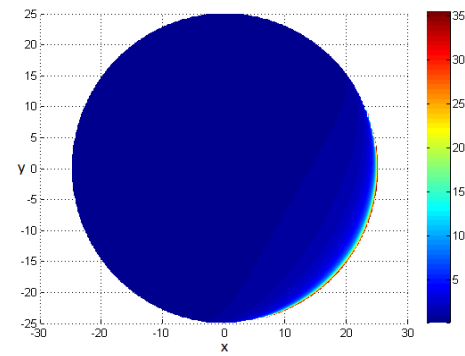


**Figure A.8:** Two Sensors:  $\phi = 0^\circ$ ,  $\theta_2 = 300^\circ$

# Appendix B

## Localization with Two Sensors: $\phi \neq 0^\circ$

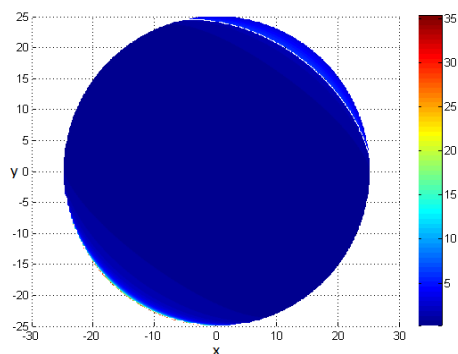


**Figure B.1:** Two Sensors:  $\phi = 30^\circ$ ,  $\theta_2 = 190^\circ$

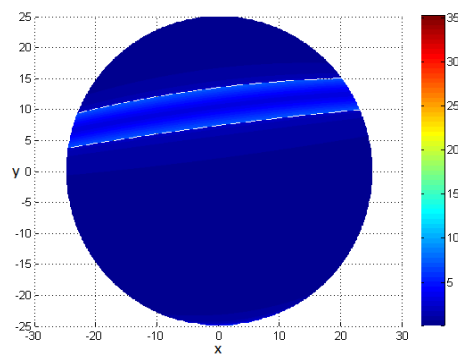


**Figure B.2:** Two Sensors:  $\phi = 50^\circ$ ,  $\theta_2 = 210^\circ$

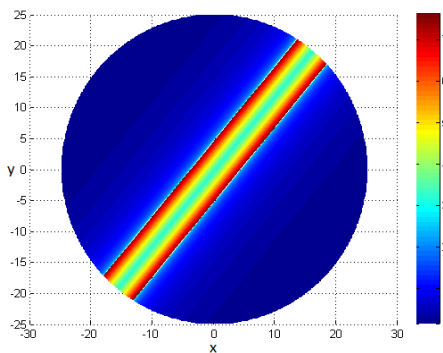


**Figure B.3:** Two Sensors:  $\phi = 70^\circ$ ,  $\theta_2 = 230^\circ$

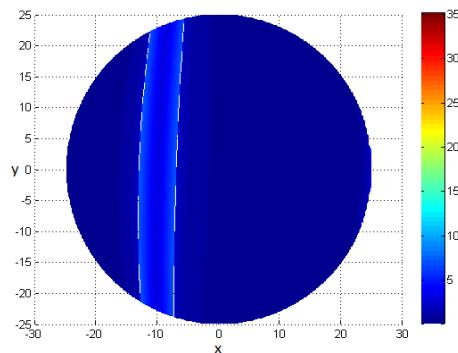


**Figure B.4:** Two Sensors:  $\phi = 20^\circ$ ,  $\theta_2 = 290^\circ$

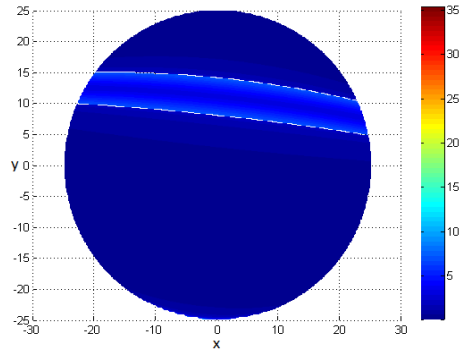


**Figure B.5:** Two Sensors:  $\phi = 40^\circ$ ,  $\theta_2 = 310^\circ$

# Appendix C

## Experiment 1 with Three sensors

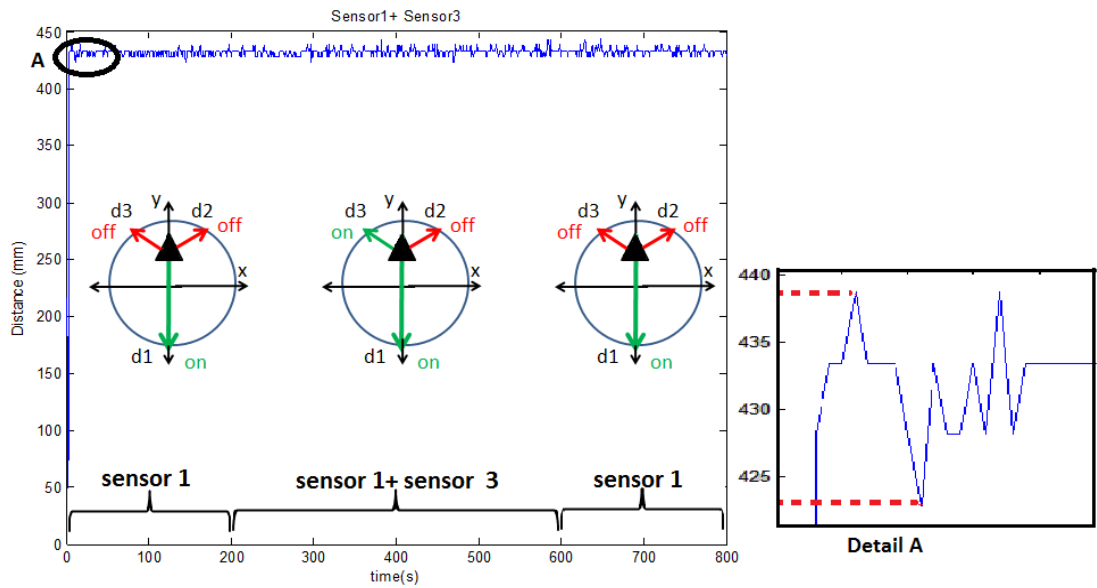


Figure C.1: Experiment 1 with Three Sensors: Sensors 1 and 3

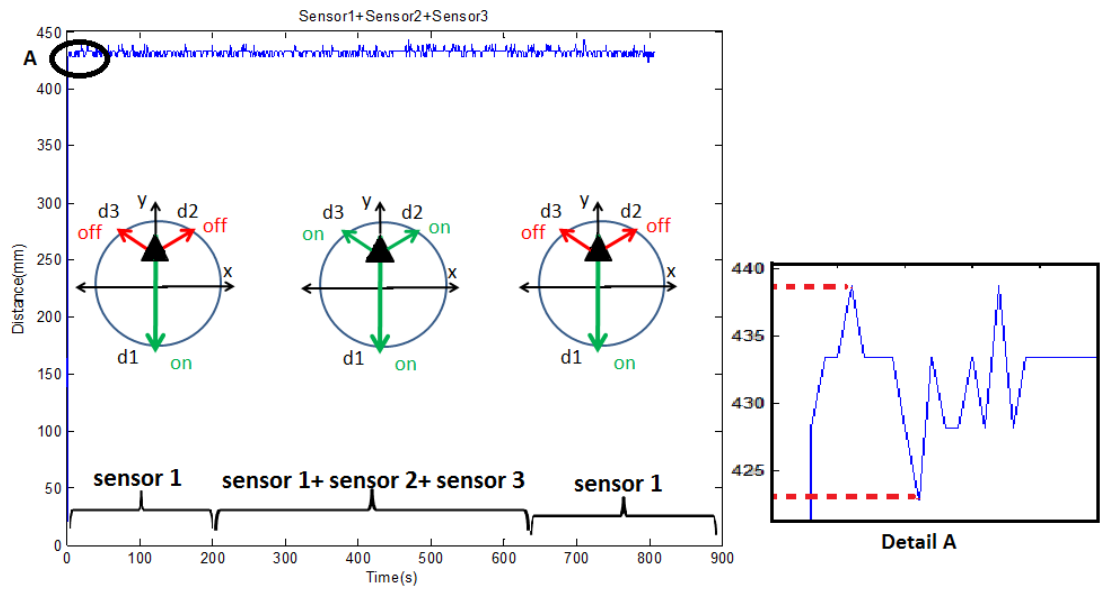


Figure C.2: Experiment 1 with Three Sensors: Sensors 1, 2 and 3

# Appendix D

## Experiment 1 with Four sensors

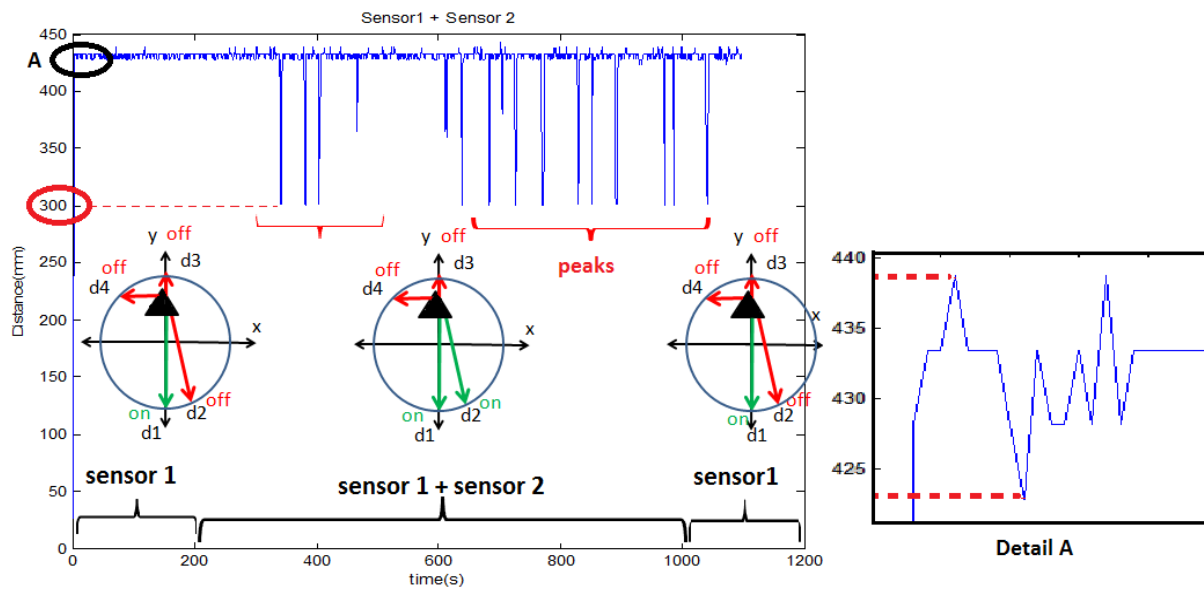


Figure D.1: Experiment 1 with Four Sensors: Sensors 1 and 2

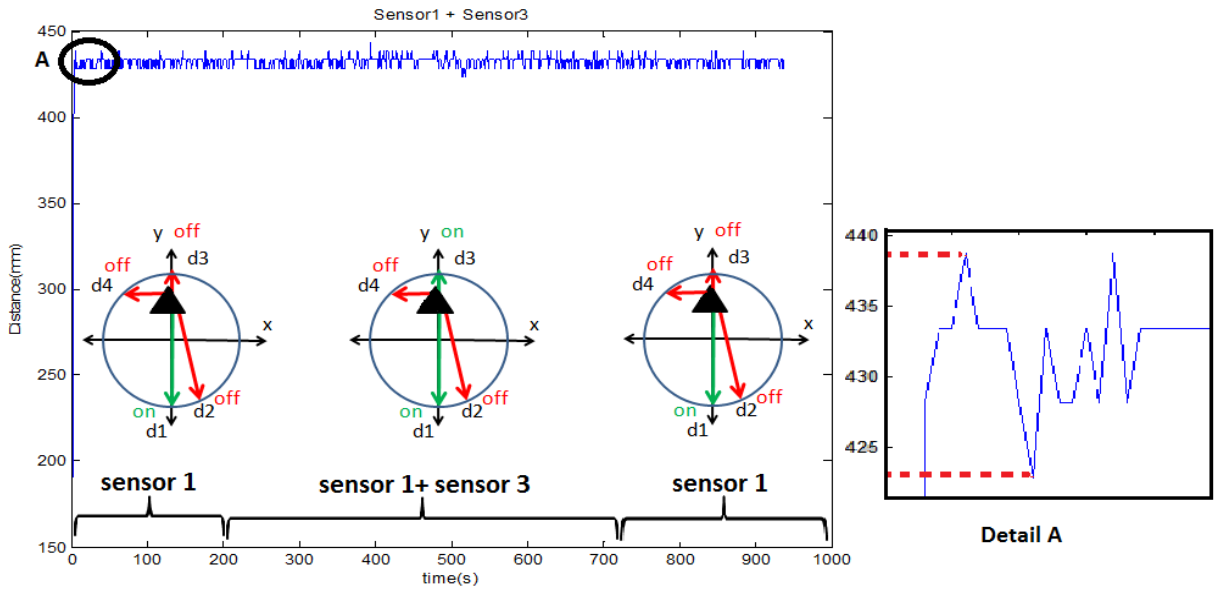


Figure D.2: Experiment 1 with Four Sensors: Sensors 1 and 3

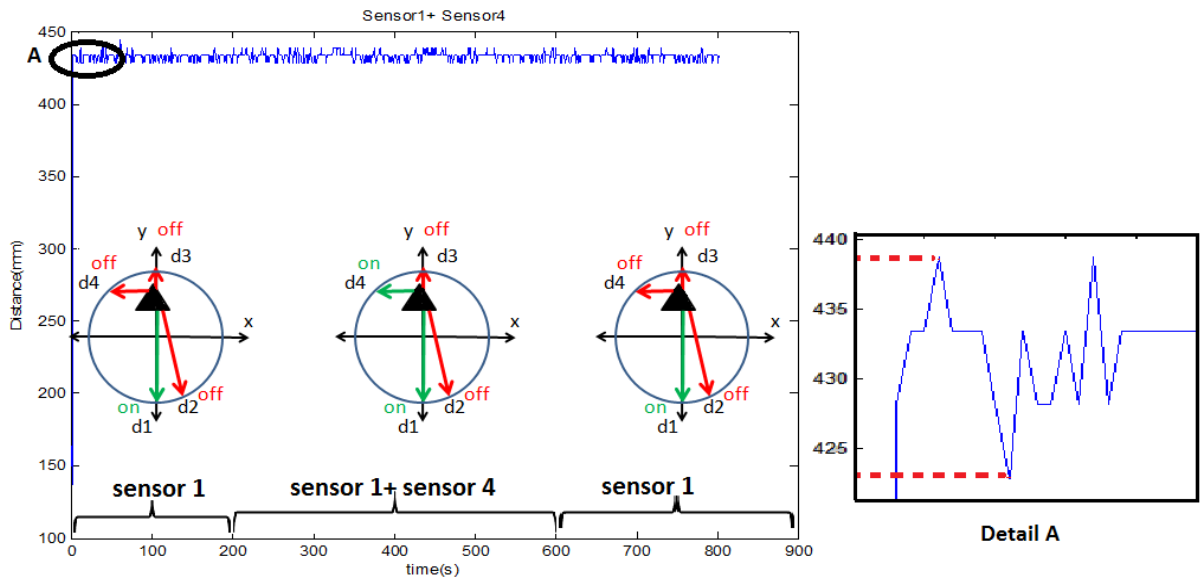


Figure D.3: Experiment 1 with Four Sensors: Sensors 1 and 4

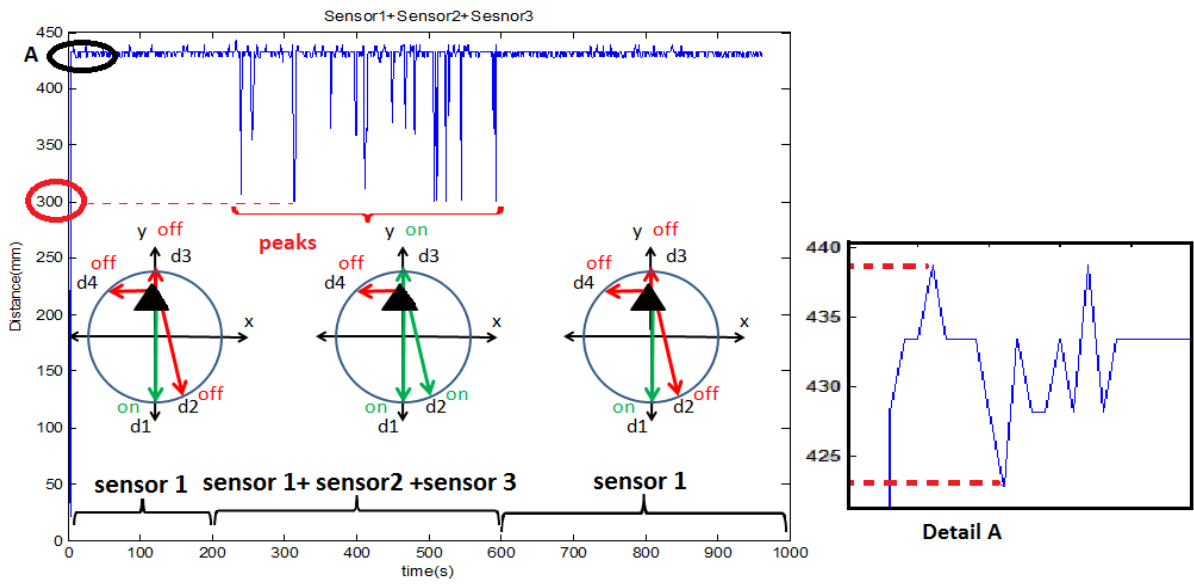


Figure D.4: Experiment 1 with Four sensors: Sensors 1, 2 and 3

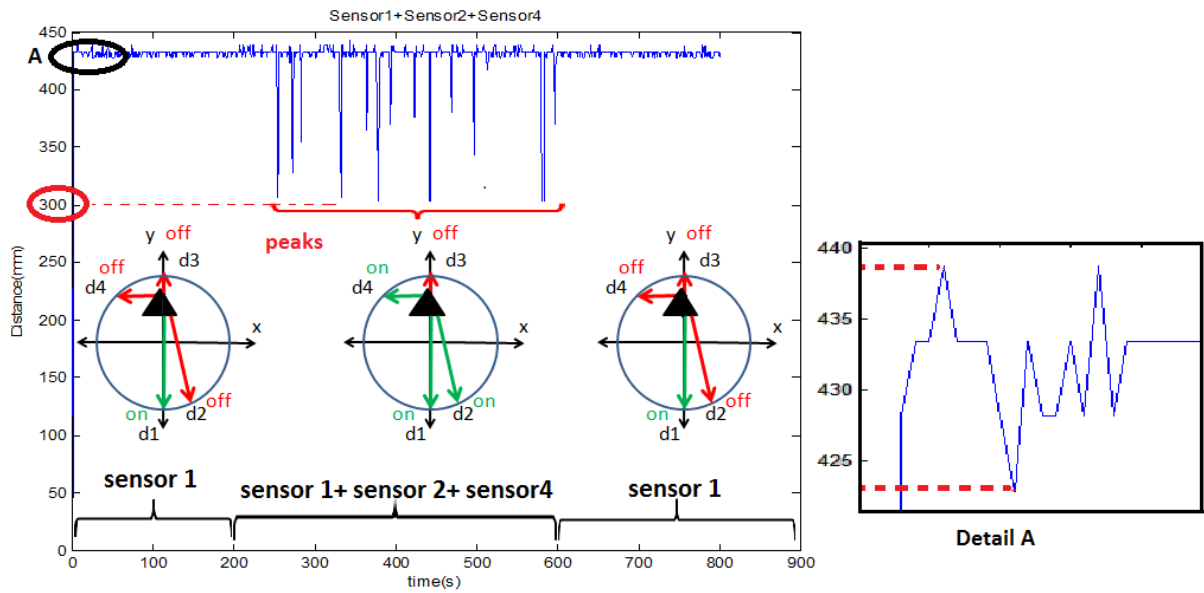


Figure D.5: Experiment 1 with Four Sensors: Sensors 1, 2 and 4

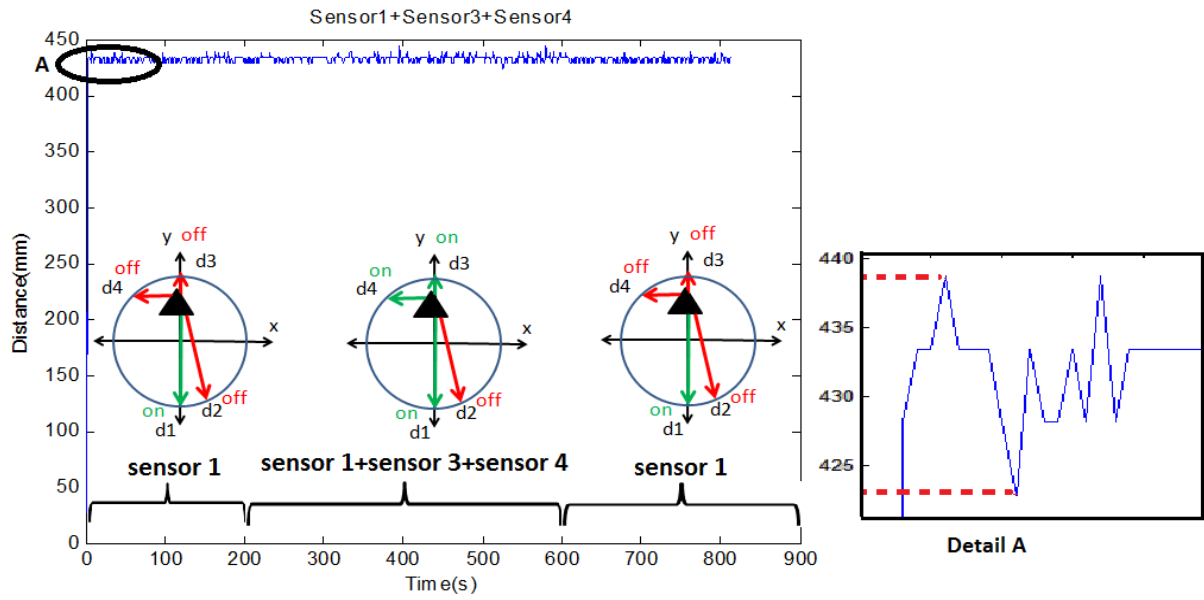


Figure D.6: Experiment 1 with Four Sensors: Sensors 1, 3 and 4

# Bibliography

- [1] P. E. Myers, “Above ground storage tanks,” McGraw-Hill Professional, 1997.
- [2] EPA-550-F-01-00, “Rupture hazard from liquid storage tanks,” Office of Solid Waste and Emergency Response, US Environmental Protection Agency, January 2001.
- [3] W. Athertron and J. Ash, “Review of failures, causes & consequences in the bulk storage industry,” University research conference, Liverpool John Moores University, United Kingdom, 2007.
- [4] A. Abdulla *et al*, “Localization of a submersible mobile inspection platform in an oil storage tank,” 7th International Symposium on Mechatronics and its Applications (ISMA), 2010.
- [5] B. Hiebert-treuer, “An introduction to robot slam (simultaneous localization and mapping),” Bachelor of Arts in Computer Science-Middlebury College, Middlebury, Vermont, USA, 2007.
- [6] L. Chen and H. Hu, “Towards localization and mapping of autonomous underwater vehicles: A survey,” technical report, School of Computer Science and Electronic Engineering University of Essex, United Kingdom, 2011.
- [7] M. J. Caruso, “Applications of magnetoresistive sensors in navigation systems,” *Readings*, vol. 72, pp. 15-21, 1997.
- [8] N. S. Reddy and J. Murray, “Transfer orbit stage gyrocompass alignment algorithm in a twist and sway environment for mars observer mission on commercial titan,” *IEEE Aerospace and Electronic Systems Magazine* (ISSN 0885-8985), vol. 6, pp. 3-7, 1991.

- [9] A. Burg *et al*, “Mems gyroscopes and their applications,” Introduction to Microelectromechanical System, 2003.
- [10] D. Zhang *et al*, “A novel wafer level hermetic packaging for mems devices using micro glass cavities fabricated by a hot forming process,” 11th International Conference on Electronic Packaging Technology & High Density Packaging (ICEPT-HDP), 2010.
- [11] J. van Deventer and J. Delsing, “An ultrasonic density probe,” *IEEE Ultrasonics Symposium*, pp. 871-876, 1997.
- [12] K. Kadoya, N. Matsunga, and A. Nagashima, “Viscosity and thermal conductivity of dry air in the gaseous phase,” *Journal of Physical and Chemical Reference Data*, vol. 14, pp. 947-970, 1985.
- [13] A. Werner *et al*, “Viscosity and phase behaviour of petroleum fluids with high asphaltene contents,” *Fluid Phase Equilibria*, vol. 147, pp. 343-356, 1998.